Applying tradespace exploration methods to remote sensing system of systems for wildfire detection and management

by

Gautam Madhivanan

B.S., Rutgers University (2013)

Submitted to the System Design and Management Program
in partial fulfillment of the requirements for the degree of

Master of Science in Engineering and Management

at the

MASSACHUSETTS INSTITUTE OF TECHNOLOGY

February 2022

Author .....
System Design and Management Program
January 14, 2022

Certified by .....
Olivier L. de Weck
Apollo Program Professor of Astronautics and Engineering Systems
Thesis Supervisor

Accepted by .....
Joan S. Rubin
Executive Director, System Design and Management Program

Applying tradespace exploration methods to remote sensing system of systems for wildfire detection and management

by

Gautam Madhivanan

Submitted to the System Design and Management Program
on January 14, 2022, in partial fulfillment of the
requirements for the degree of
Master of Science in Engineering and Management

Abstract

In recent years the world has seen wildfires cause an increasing amount of damage and take more human lives. Studies have shown that this is a result of climate change, which is only going to get worse as time goes on. Currently, firefighting teams have limited access to technologies that could help them reduce the damage of wildfires. Both the firefighting and fire science community have shown interest in using drones and satellites to help with the fire detection and fire management efforts. Both drones and satellite have various tradeoffs when being used for remote sensing applications. To determine what combinations of sensors would best suit the needs of the firefighting and fire science communities, this project conducts a trade study where the relative utilities and cost of the combined systems can be compared. Four phases of the candidate systems operation were identified, fire prediction, fire detection, fire monitoring, and fire damage assessment. Each of these operational phases were used to determine the overall utility of the candidate system. Additionally, the Camp fire (California, 2018) was used as a reference fire to evaluate the utility during each of these phases. It was found that a system of systems comprised of multiple geosynchronous satellites and aircraft would be the optimal system at a cost of 518 million USD. This system would use the geosynchronous orbiting satellites primarily for prediction, detection and damage assessment. The aircraft would primarily be used for monitoring active fires. While this study was focused on the support of one large fire in the western U.S., to support additional areas additional satellites or aircraft could be added as needed.

Thesis Supervisor: Olivier L. de Weck
Title: Apollo Program Professor of Astronautics and Engineering Systems

Acknowledgments

It is with a bittersweet feeling that I complete my time at MIT. During my time here, my expertise in engineering and management has grown exponentially. This was by no means an easy effort, in part due to the global pandemic and its side effects. I would like to thank the SDM program for giving me the opportunity to grow as I have. This program has completely changed the way I look at engineering complex systems. I'm extremely grateful for my advisor Professor Olivier de Weck, whose kind and insightful support made this thesis possible. I will continue to use what I have learned in my coursework and during this study through the rest of my career.

Thank you to my colleagues Chris Brundgardt and Don Granquist-Fraiser, for answering my frequent barrages of questions and for your support during this study. Thank you to my colleagues Guy Smith, Khaled Genidy, Roy Bean, Zi Wang, and Joe Doucette, for all your support through this program. I'd like to thank Raytheon Technologies, for their commitment to the growth of their employees. I'd also like to thank Kurtis Nelson from USGS, for your insight into the field of fire management.

Finally, I'd like to thank my family. I'd like to thank my grandparents, for their dedication to their grandchildren's education, and for everything which they passed on to all the subsequent generations. I'd like to thank my parents, for their love, support, and encouragement throughout this program. Lastly, I'd like to thank my partner, Julia Dougherty, for too many things to list.

Contents

1 Introduction **21**

1.1 Climate Change 22

1.2 The Camp Fire 23

1.3 Yarnell Hill 24

1.4 Research Problem 25

2 Fire Science **27**

2.1 Fire Ignition and Spread 27

2.2 Fuel Measurement 29

2.2.1 Vegetation and Moisture Indices 30

2.3 Fire Detection 32

2.4 Fire Monitoring and Prediction 33

2.5 Post Fire Recovery 34

3 Remote Sensing **37**

3.1 Focal Plane Arrays 38

3.2 Optics 42

3.3 Sensor Systems 45

3.4 Ground Stations 49

3.5 System of Systems 50

4 Methods **53**

4.1 Tradespace Analysis 53

4.1.1 Understand the Problem statement . . . 53
4.1.2 Identify Stakeholders . . . 54
4.1.3 Identify and Weight Decision Factors . . . 54
4.1.4 Identify and Weight Decision Factor Criteria . . . 55
4.1.5 Characterize Utility Functions . . . 55
4.1.6 Identify Viable Candidate Solutions . . . 55
4.1.7 Evaluate Candidate Solution Decision Criteria . . . 55
4.2 Utility vs Cost . . . 55

5 Stakeholder Needs **57**
5.1 Interviews . . . 57
5.1.1 United States Geological Survey . . . 57
5.2 Panels . . . 58
5.2.1 The Power of Real-Time Data for Firefighting . . . 58
5.2.2 Hot Mess: Remote Sensing Applications for Wildfires and Other Natural Disasters . . . 60

6 Model **63**
6.1 Design Constraints and Assumptions . . . 63
6.2 Input Parameters . . . 64
6.3 Input Variables . . . 65
6.3.1 Altitude . . . 66
6.3.2 GSD . . . 66
6.3.3 Pixel Pitch . . . 67
6.3.4 Crosstrack Pixels . . . 67
6.4 System Design . . . 67
6.4.1 Spaceborne Sensors . . . 69
6.4.2 Airborne Sensors . . . 72
6.4.3 Ground Station . . . 74
6.4.4 Cost . . . 75
6.4.5 Utility Function . . . 77

6.4.6 Multiple Systems 79
6.4.7 Mixed Systems 80

7 Analysis **81**
7.1 Prediction Utility 81
7.2 Detection Utility 84
7.3 Monitoring Utility 86
7.4 Assessment Utility 88
7.5 Overall Utility 90
7.5.1 Other Wavelengths 92
7.6 Comparison to Current and Other Systems 97

8 Conclusion **101**
8.1 Findings 101
8.2 Future Work 103

A Figures **105**
A.1 Orbital Paths 105
A.2 Utility Curves 106

List of Figures

1-1 U.S. Federal Fire Suppression Cost [12] 22
1-2 Total Fires and Acres Burned in the U.S. [12] 23
1-3 Campfire Mapping 24

2-1 Wildland Fire Growth [55] 28
2-2 Wildfire Types [51] 29
2-3 Ignition Probability vs Moisture for different Trees [55] 30
2-4 Normalized Difference Vegetation Index [23] 31
2-5 Osborne Firefinder [28] 32
2-6 Cold Springs Fire DNBR from LandSat 8 data [20] 35

3-1 Light Spectrum and Atmospheric Transmittance [17] 38
3-2 Focal plane array example [60] 40
3-3 Visible, MWIR and LWIR looking through fog [35] 42
3-4 Cassegrain Telescope Optics of the Hubble Space Telescope (HST) [39] 43
3-5 Ground Sample Distance [44] 44
3-6 Instantaneous Field of View [56] 45
3-7 Gimballed Sensor Systems and their Ground Tracks for different Instruments [56] 46
3-8 Remote Sensing Platform Examples: GEO Satellite (Top Left), LEO (Top Right), UAV (Bottom Left), Fire Tower (Bottom Right) 48
3-9 Ground Segment [41] 50

4-1 Generic Tradespace with Pareto Frontier [30] 56

6-1 Multiple (left), Mixed(center), Multiple and Mixed (right) 80

7-1 Fire Prediction Utility 84
7-2 Fire Detection Utility 86
7-3 Fire Monitoring Utility 88
7-4 Post-Fire Assessment Utility 89
7-5 Overall Utility 92
7-6 Red Band Overall Utility 94
7-7 MWIR Overall Utility 95
7-8 LWIR Overall Utility 97
7-9 Overall Utility Comparison to Other Systems 99

A-1 Orbital path of 200km 45 degree inclination LEO Satellite Candidate 105
A-2 Orbital path of 2000km 45 degree inclination LEO Satellite Candidate 106
A-3 Prediction Imaging Rate Utility 106
A-4 Prediction TTA Utility 107
A-5 Prediction Availability Utility 107
A-6 Prediction GSD Utility 108
A-7 Prediction DL Utility 108
A-8 Detection Imaging Rate Utility 109
A-9 Detection TTA Utility 109
A-10 Detection Availability Utility 110
A-11 Detection GSD Utility 110
A-12 Detection DL Utility 111
A-13 Monitoring Imaged Area Utility 111
A-14 Monitoring TTA Utility 112
A-15 Monitoring Availability Utility 112
A-16 Monitoring GSD Utility 113
A-17 Monitoring DL Utility 113
A-18 Assessment Imaging Rate Utility 114
A-19 Assessment TTA Utility 114

A-20 Assessment Availability Utility 115
A-21 Assessment GSD Utility 115
A-22 Assessment DL Utility 116

List of Tables

3.1 Infrared Bands 41
3.2 Satellites Commonly used for Fire Science 49

4.1 Stakeholders 54

6.1 Input Variables 66
6.2 Revisit Time 70
6.3 Spaceborne Sensor Aperture and Weight 71
6.4 UAV Platforms as a benchmark 72
6.5 Airborne Sensor EFL and Weight 74
6.6 Fire Prediction and Detection Utility Parameters 78
6.7 Monitoring and Post-Fire Assessment Utility Parameters 79

7.1 LEO Candidates' Prediction Utility 82
7.2 Airborne Candidates' Prediction Utility 83
7.3 GEO Candidates' Prediction Utility 83
7.4 Candidates' Detection Utility 85
7.5 Candidates' Monitoring Utility 87
7.6 Candidates' Assessment Utility 89
7.7 Candidates' Overall Utility 90
7.8 Index 3634 Systems 91
7.9 Candidates' Red Overall Utility 93
7.10 Candidates' MWIR Overall Utility 95
7.11 Candidates' LWIR Overall Utility 96

7.12 Index 6867 Systems 97

Acronyms and Variables

IR	Infrared
NIR	Near Infrared
SWIR	Short Wave Infrared
MWIR	Mid Wave Infrared
LWIR	Long Wave Infrared
NIROPS	National Infrared Operations
IHC	Interagency Hotshot Crew
LMFC	Live Fuel Moisture Content
NDVI	Normalized Difference Vegetation Index
GNDVI	Green Normalized Difference Vegetation Index
NDWI	Normalized Difference Water Index
NBR	Normalized Burn Ratio
DNBR	Differenced Normalized Burn Ratio
LEO	Low Earth Orbit
GEO	Geosynchronous Equatorial Orbit
FARSITE	Fire Area Simulator

RAWS Remote Automatic Weather Station

UAV Unmanned Aerial Vehicle

UAS Unmanned Aircraft Systems

BAER Burned Area Emergency Response

BAES Burned Area Emergency Response Specialist

FASMEE Fire and Smoke Model Evaluation Experiment

RADAR Radio Detection And Ranging

LIDAR Light Detection And Ranging

IMU Inertial Measurement Unit

GPS Global Positioning System

CMOS Complementary Metal Oxide Semiconductor

CCD Charge Coupled Device

RGB Red Green Blue

b Constant of Proportionality

GSD Ground Sample Distance

IFOV Instantaneous Field Of View

FOV Field Of View

EFL Effective Focal Length

SoS System of Systems

EIRP Equivalent Isotropic Radiated Power

FSPL Free Space Path Loss

ESA Electronically Steerable Antennas

SNR Signal to Noise Ratio

MODCOD Modulation and Coding

SWAP Size Weight and Power

INCOSE International Council on Systems Engineering

SEBOK Systems Engineering Book Of Knowledge

ROM Rough Order Magnitude

USGS United States Geological Survey

WFDSS Wildland Fire Decision Support System

HAPS High Altitude Platform System

EOIR Electro-Optical/Infrared

AI Artificial Intelligence

SAR Synthetic Aperture RADAR

MTBO Mean Time Between Overhaul

OT Overhaul Time

Re Radius of the Earth

T Orbital Period

SLOC Software Lines Of Code

Alt Altitude

FUEGO Fire Urgency Estimator on Geosynchronous Orbit

acTAT Aircraft Turnaround Time

FTE	Full Time Engineer
g	growth factor
x	mean value
k	rising or falling constant

Chapter 1

Introduction

The 2020 California wildfires resulted in over 30 deaths, destruction of over 10 thousand structures, and cost over 12 billion dollars in the Golden State alone [26]. The cost of wildfire suppression has increased continually over the past several decades as seen in figure 1-1. Due to climate change, fire seasons are only expected to get longer and more damaging. As fire seasons expect to see more severe fires that encompass more burned area and more property damage, minimizing the damage caused by wildland fires become increasingly important. Currently satellites and aircraft are used to support the detection and management of wildland fires. These are often multipurpose systems, limited in quantity, and sometimes on loan during specific events. To prepare for future fire seasons, a robust and persistent system of systems is needed that prioritizes the needs of those fighting fires.

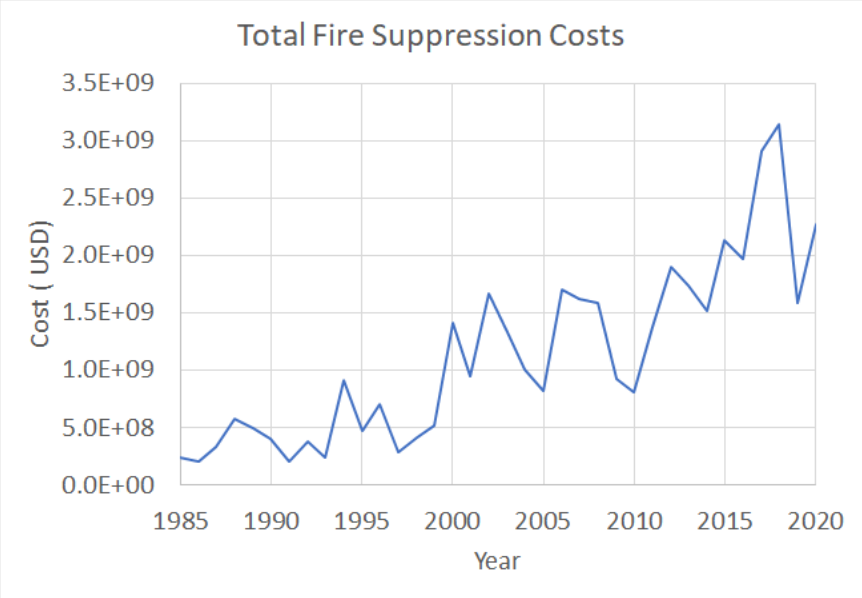

Figure 1-1: U.S. Federal Fire Suppression Cost [12]

1.1 Climate Change

The 2017 fire season saw 622,000 hectares of burned area globally compared to an average of 228,000 hectares in previous years [18]. While 2017 was a particularly bad fire season, it is clear that the areas burned in recent fire seasons have been trending upwards. Interestingly, the total number of fires that are occurring in the U.S. don't seem to be trending upwards in a similar manner as seen in figure 1-2. The reason for this has to do with the fact that we have been consistently breaking global heat-wave records. This has resulted in longer periods with dry heat, leading to increasing droughts all over the globe. A recent study found that the temperature extremes which caused the higher than average burn area seen in recent fire seasons was "virtually impossible without human-caused climate change" [54]. Since climate change is expected to result in increasingly high global temperatures, it can be assumed that fires are also going to increase in severity.

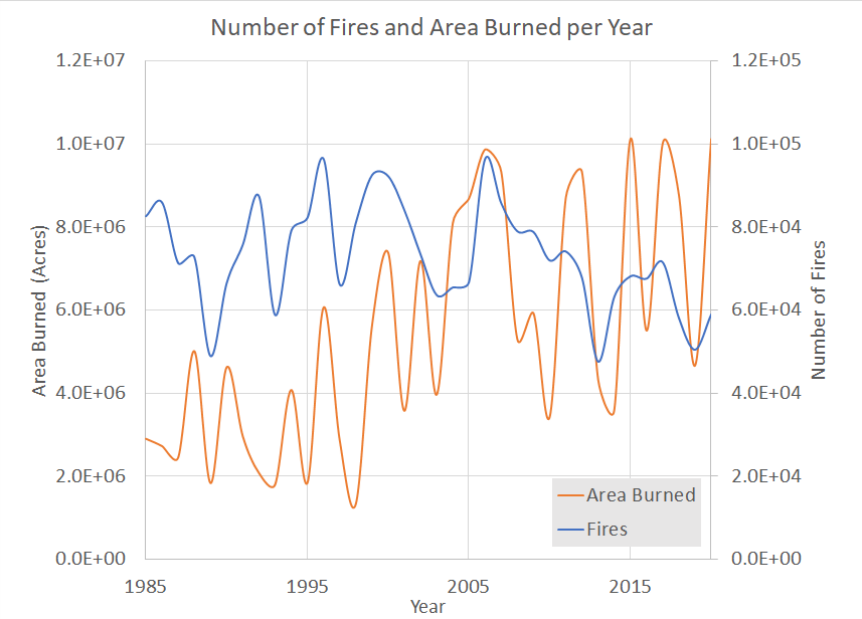

Figure 1-2: Total Fires and Acres Burned in the U.S. [12]

1.2 The Camp Fire

The wildfire referred to as the "Camp fire" started in Butte County, California on November 8th 2018. Prior to ignition, there was a 200 day period with almost no precipitation. This resulted in drier vegetation as well as an accumulation of fallen pine needles on the forest floor, which meant there was a higher than average amount of fuel for a potential fire. The fire was initially reported through 911, and was approximately 30 square meters. The fire engines took 10 minutes to reach the fire for the initial size up. Twenty minutes after the first fire was reported, a second ignition occurred. About 1.5 hours after the first fire was reported aircraft support was providing information on the fire conditions and rate of spread. Smoke and wind made it difficult for the air support personnel to provide information on the fire conditions and spread. Additionally, fire spotting, where fires start beyond the fire front, made it hard to gain an accurate rate of spread. The LandSAT 8 satellite overflew the area later in the day and was able to provide imagery in the visible and short wave infrared bands. Additionally, an aerial infrared perimeter mapping was done the same day, after the satellite imagery was acquired. It was found that the

LandSAT satellite contained more detail than the aerial IR perimeter mapping. The rate of spread of the fire was such that it quickly spread beyond the initial perimeter that was found through the IR mapping. Infrared flights continued for multiple days during the fire, mapping up to nearly 34,000 acres in a day. The IR perimeter mapping flights helped understand the extent of the fire as it progressed into other areas. Figure 1-3 shows the mapping done by the LandSat8 satellite and a National Infrared Operations (NIROPS) aircraft. The LandSat8 imagery was taken using data from the red, green, blue, and short wave infrared (SWIR) bands on November 8, around 10:45 am. [21]. The NIROPS imagery was taken using mid wave infrared (MWIR) and long wave infrared bands (LWIR) on November 8, 5:54 pm [50].

The Camp fire was fully contained 18 days after it was first reported. The fire resulted in 85 fatalities, over 18,000 destroyed structures and 153 336 acres consumed. The estimated cost of losses is 16.6 billion dollars with an additional 3 billion dollars of clean up. This made the camp fire one of the deadliest and most destructive fires in California history. [47]

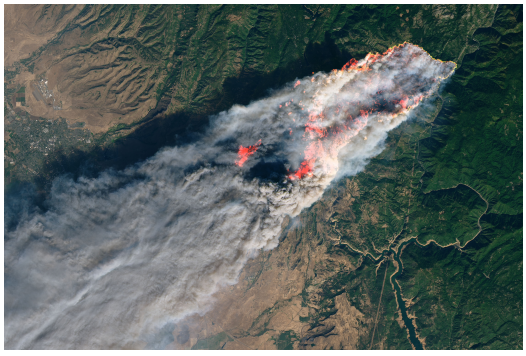

(a) LandSat8 Satellite [21]

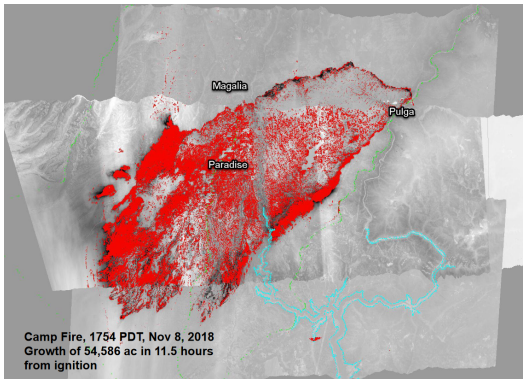

(b) NIROPS Aircraft [50]

Figure 1-3: Campfire Mapping

1.3 Yarnell Hill

The Yarnell Hill fire started on June 28, 2013 and was one of multiple fires started by a lightning storm near Yarnell, Arizona. Prior to the fire there was a long drought period during the summer resulting in a high fire severity environment due to critically low

fuel moisture content. Multiple parties notified the fire dispatch of lightning ignited fires. Upon initial sizeup, the fire was reported to be less than an acre in size. Air attack noted that the fire had very little smoke, and that there were no additional fires. The following day, June 29, air attack is used to check the effectiveness of the retardant dropped on the fire. Later in the day the fire continues to grow and results in more smoke output. The additional smoke caused the air attack to have difficulty assessing the fire behavior, but they reported the flame spreading at a rate of 330 to 660 feet per hour. The next day , June 30, an interagency hotshot crew (IHC) was deployed to establish an anchor point near a part of the fire. Later in the day, the winds changed driving the fire in the direction of the IHC. The air attack communicated this information to the fire management. After this, the air attack had to leave the firefighting effort due to time limitation which stipulated that aircraft can only fly for 8 hours a day and be on the clock for 14 hours a day. The air attack performed a handoff to allow another aircraft to take over their air attack duties. The air attack and the management were under the perception that the IHC were in a good spot, but the IHC were overtaken by the fire resulting in the loss of 19 firefighters lives. [16]

1.4 Research Problem

It is clear that there is a gap between the current capabilities of wildfire management and the capabilities needed to meet the current/future demands. Specifically, firefighting personnel need a better way to predict, detect, monitor and assess the damage from wildfires because every year, the damage from wildfires increases. This study will look into the use of remote sensing systems to support wildfire management efforts in the four aforementioned phases (Prediction, Detection, Monitoring, Damage Assessment). The structure of the study is as follows:

- Chapter 1, Introduction: Multiple significant wildfires are detailed, as well as the effect of climate change on the increasing damage of wildfires.

- Chapter 2, Fire Science: The field of fire science is reviewed, with specific attention to the four phases of wildfire management.
- Chapter 3, Remote Sensing: The field of remote sensing is reviewed, with specific attention to passive optical airborne and spaceborne systems.
- Chapter 4, Methods: Tradestudy methodology is reviewed including tradespace analyses, Pareto Frontier and utility functions.
- Chapter 5, Stakeholder Needs: Interviews and panels are presented on the topic of remote sensing in wildfire management.
- Chapter 6, Model: The model is detailed including details on the utility and cost functions.
- Chapter 7, Analysis: The outputs of the model are analyzed.
- Chapter 8, Conclusion: The significance of the findings are reviewed.

Chapter 2

Fire Science

2.1 Fire Ignition and Spread

It takes three separate components to start a fire; oxygen, fuel, and an ignition source, generally in the form of heat. Plants are capable of producing two of the three components; fuel and oxygen. While historically the heat source was produced exclusively by lightning, in current day lightning is only one of many possible heat sources. When heat is applied to the fuels (specifically organic fuels) the heat drives off the moisture within the fuel and compounds within the fuel become flammable gasses. This process of dehydration and conversion of solid fuel to gaseous fuel is referred to as pyrolysis. The resulting gaseous fuel reacts exothermically with oxygen when mixed at specific ratios which is referred to as combustion. There are two separate temperatures that are important for ignition of a fire, the auto-ignition temperature and the pilot ignition temperature. The pilot-ignition temperature is the temperature which the fuel will ignite when subjected to an ignition source, while the auto-ignition temperature is the temperature at which the fuel will ignite even without the ignition source. The lower these temperatures for a fuel, the higher the chance of ignition (given the right mixture of fuel and oxygen). These temperatures are lowered for a fuel as it loses moisture. Once ignition occurs, since combustion is exothermic it heats up any neighboring fuel. If enough pyrolysis occurs, the neighboring fuel can ignite resulting in growth of the fire. After the inception of the fire, the flame begins to

move outward from the center leaving a scorched center where the fuel was exhausted. The leading edge of the fire is referred to as the flame front, as seen in figure 2-1. The presence of wind results in the spread of the fire being oblong instead of circular, where the movement of the flame front is faster on the side along the wind vector. Elevation can also affect the spread of the fire. [55]

Figure 2-1: Wildland Fire Growth [55]

When the embers from one fire move past the flame front and ignite a separate fuel source it is referred to as a spot fire. In wildland fire there are multiple methods by which the fire could spread, as shown in figure 2-2. The fire could burn beneath the forest surface, which is called a ground fire. The surface of the forest including

leaves and fallen branches could burn, which is referred to as a surface fire. Finally the canopy of the forest can burn, which is referred to as a crown fire. Transition from one mode to another can be fast and dangerous. When air temperature and wind speed quickly rise, and humidity drops, a flashover can occur where the fire quickly transitions from a surface fire to fire engulfing everything from the surface to the canopy. Another dangerous occurrence is when additional air is added to a smoldering fire providing enough oxygen for the flammable gases to ignite causing an explosion known as a backdraft.

There are four ways to put out a fire. The heat of the fire can be cooled, the oxygen can be removed from the fire, the fuel can be removed, or the chemical reaction can be broken. Water dropped on a fire can cool the fire, enough of it can reduce the oxygen available to the fire. Fire retardants reduce the flammability of fuels mitigating the chemical reaction of fire. Creating firebreaks, where forest is removed to prevent the fire from progressing and controlled burns are methods of removing the fuel.

Figure 2-2: Wildfire Types [51]

2.2 Fuel Measurement

Determining where and when a wildfire will occur and how much damage it could cause can be a difficult endeavor. This is due to size of the area where the fire could occur being so large and the size at which fires can start being so small. Since the three requirements for a fire are oxygen, fuel and heat, it is necessary to need to look

at all three to make estimations. The local ambient temperature can be measured to estimate the heat using a variety of methods. Oxygen is normally measured in the form of wind velocity using an anemometer. Fuel comes in a variety of shapes and sizes as well as varying based on location so it can be a bit trickier to measure. One way to measure the capacity of fuel is through live fuel moisture content (LFMC) or Fuel Moisture Content (FMC) [37]. Since dehydration is necessary before combustion, a higher amount of moisture in a material requires more work to be done for combustion to occur. The relationship between moisture and ignition probability depends on the type of vegetation, as shown in figure 2-3. Some earth observation satellites, like the soil moisture active passive (SMAP) mission, measure the moisture in the soil. This alone is not a good predictor of vegetation combustibility, but when combined with surface temperature and vegetation indices can be a holistic predictor of future wildland fires [40].

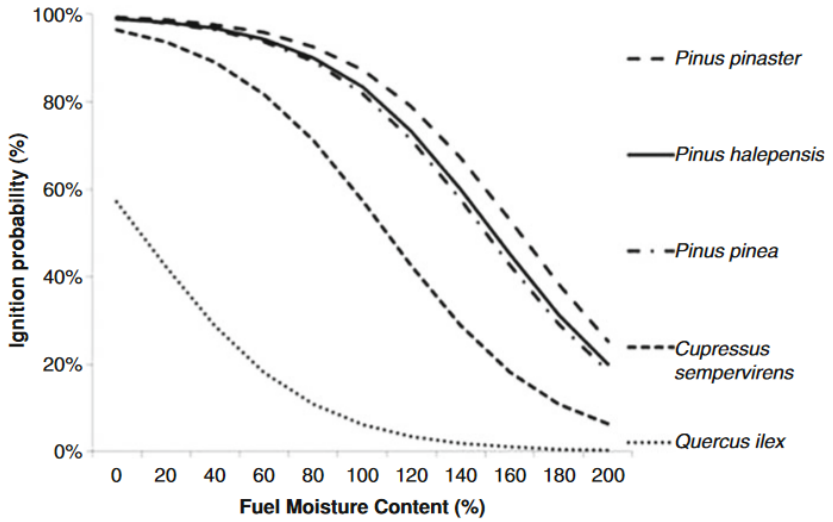

Figure 2-3: Ignition Probability vs Moisture for different Trees [55]

2.2.1 Vegetation and Moisture Indices

One way of characterizing live fuel moisture is through vegetation or moisture indices. These indices are relationships between multiple spectral values from an area, as seen in figure 2-4. The Normalized Difference Vegetation Index (NDVI) , Green Nor-

malized Difference Vegetation Index (GNDVI), Normalized Burn Ratio (NBR), and Normalized Difference Water Index (NDWI) are all examples of vegetation indices. These indices compare light from the red, green, and short wave infrared (SWIR) band respectively to the near infrared (NIR) band. The equation for the NDWI can be seen in equation 2.1

$$NDWI = \frac{NIR - SWIR}{NIR + SWIR} \tag{2.1}$$

The difference between the two wavelengths compared can be used to determine the health of the plant life in the target area. This information is normally acquired from the data coming out of earth observation satellites. Since the earth observation satellites pass over the same area on a regular basis, the data from the most recent passover can be used to generate the vegetation indices. If data for the same index is obtained from shortly before a fire and shortly after a fire, the difference between the two time intervals can create a differenced index like Differenced Normalized Burn Ratio (dNBR). [37]

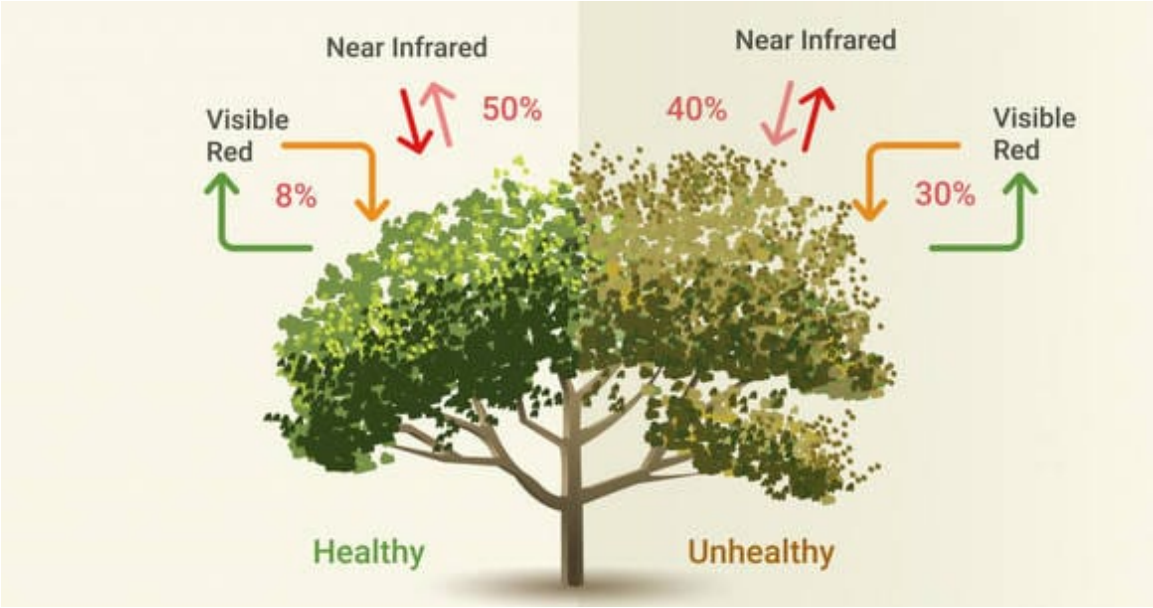

Figure 2-4: Normalized Difference Vegetation Index [23]

2.3 Fire Detection

A Review on Early Forest Fire Detection Systems using Optical Remote Sensing was performed. The typical method of fire detection involves fire watch towers, which are elevated stations placed within the forest that allow 360 degree viewing of the forest. The watch is consistently staffed with a person to monitor the forest for fires. Fires are meant to be spotted via their binoculars, usually through the presence of smoke. Then using an Osborne fire finder, shown in figure 2-5, which is essentially an alidade, the line of sight distance to the fire can be determined and placed on a map.

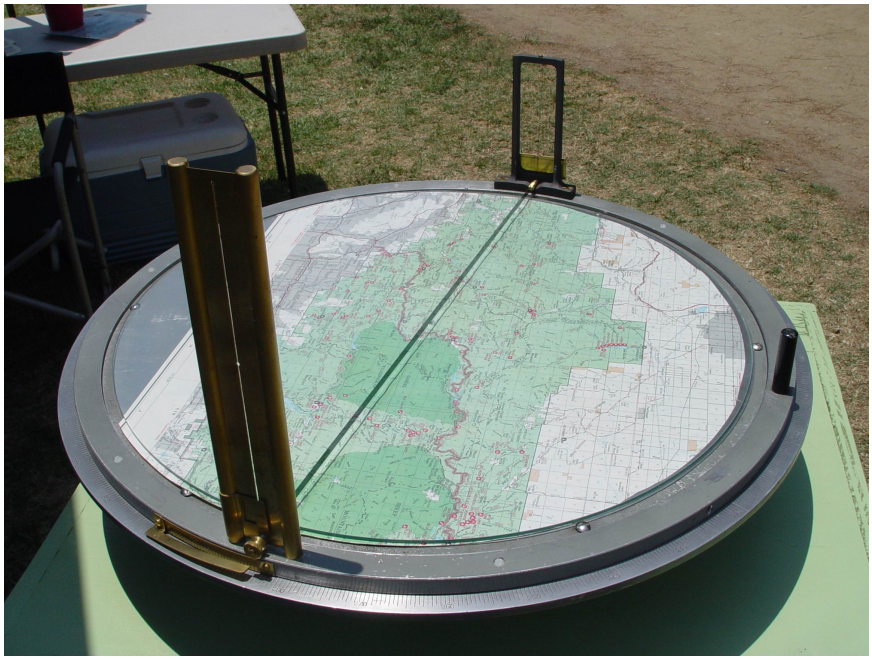

Figure 2-5: Osborne Firefinder [28]

Automated terrestrial fire detection can be done with 360 degree cameras placed at elevated locations like within fire watch towers. These cameras can be equipped with optical cameras, infrared cameras, or both. One of the limitations of terrestrial fire detection is its spatial accuracy due to the fact that these observations are made close to the ground and that they are witnessing the byproduct of the fire instead of the fire itself. So, in order to determine the best location for a slurry drop (the fire retardant dropped by wildfire fighting tanker aircraft), another measurement would need to be taken. Additionally, while fire watch towers do have a wild field of view, they are

limited in the coverage that they can provide due to their stationary nature. This can be overcome by placing the optical and infrared cameras on an aerial or spaceborne system. The downside of satellites is that low earth orbiting (LEO) satellites usually don't orbit at a high enough frequency to quickly detect fires, and most geostationary satellites don't have the sensitivity or angular resolution necessary to detect fires early. Airborne systems, on the other hand, are expensive to keep in the air continuously to detect any fires, but if fires are suspected after a lightning storm, airborne systems might still be useful.

There are multiple methods used to detect fires. Using either solely IR or visible wavelength cameras can result in a relatively high false positive rate especially if the system is expected to perform at different light levels [32]. At night the lack of radiation from the sun results in minimal light being reflected that the visible wavelength camera could detect. In the daytime a visible camera could diagnose a fire by finding pixels that are more red than blue or green. Conversely in the night, the heat from the fire would stand out more from the cooler surrounding environment while in the daytime the ambient temperature is higher making it harder to differentiate between a hotspot and the noise floor.

2.4 Fire Monitoring and Prediction

Once a fire is detected there are multiple algorithms like FARSITE which can be used to predict the spread [38]. One of the key inputs into the the model are vegetation indices. While this information can be collected prior to the fire, and input into the model, the model is not without error. Changes in fire modality can result in another model being needed. Different models are also needed to predict spot fires and other fire behavior that could change the result of the original model. Remote automatic weather stations (RAWS) are weather stations meant to be placed every 5 km apart and that are capable of measuring wind speed, fuel moisture, and temperature among other things [33] . The data from each RAWS is uplinked to a geostationary satellite and downlinked to a ground station. Similar to the fire watch towers, RAWS are

stationary and are limited in coverage. Aircraft can be used to visually chart the perimeter of an active fire and estimate its rate of spread. Visually sighting the fire can be difficult though, due to the presence of smoke or high winds. There are also remote sensing technologies which are being developed that can provide consistent high spatial resolution data for modelling, but uptake has been slow. Monitoring done by remote sensing would allow for more precise water drops via tanker aircraft. Certain new systems, like the one proposed by the MikaFire project use UAVs to precisely drop retrievable water balloons directly on the fire location [8]. Monitoring via remote sensing could provide fire location and intensity data directly to such a system to most effectively utilize high concentration and high precision water drops. Mixing airborne, spaceborne and ground based remote sensing techniques could provide a wealth of information about a fire. Collaborative efforts, like the Fire and Smoke Model Evaluation Experiment (FASMEE), are currently looking into incorporating these multiple forms of remote sensing to better understand fire behavior [4].

2.5 Post Fire Recovery

After a wildfire has done damage to a given landscape, the extent of the damage done needs to be assessed. One of the groups doing this is the U.S. Geological Survey, who uses remote sensing to calculate the Differenced Normalized Burn Ratio (DNBR), shown in figure 2-6. This is done at 30m spatial resolution for fires greater than 500 acres in the eastern U.S. and greater than 1000 acres in the western U.S. [14]. A ratio of -1.00 indicates complete destruction, while a ratio of +1.00 shows areas that are unaffected. This information is used by Burn Area emergency response (BAER) teams to determine action to minimize further damage and bring the area back into normalcy [15][10].

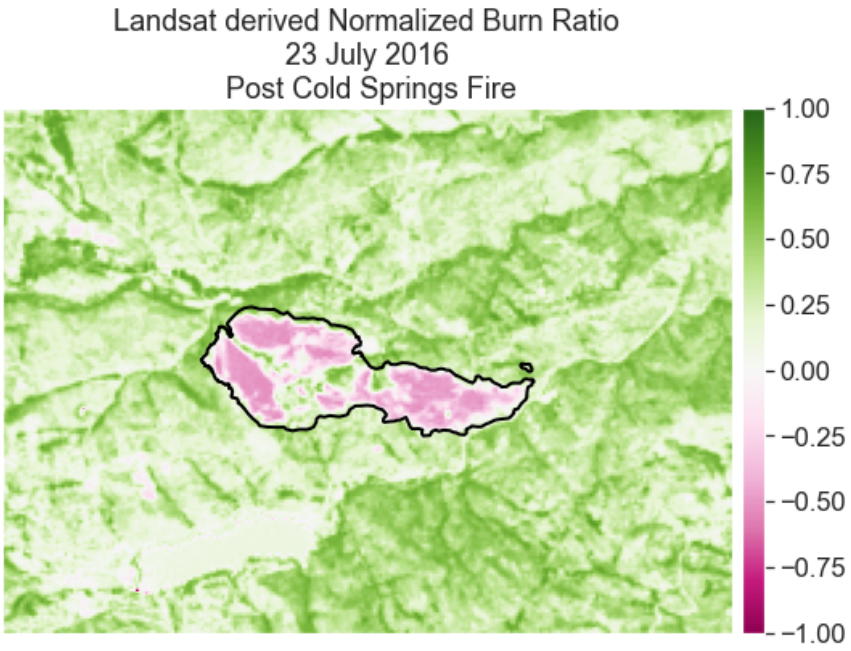

Figure 2-6: Cold Springs Fire DNBR from LandSat 8 data [20]

Chapter 3

Remote Sensing

Remote sensing is the process of taking measurements of an object from a distance. Since the object being measured is not in the immediate proximity of the sensing equipment, the sensing equipment at a distance relies on information that can be propagated through the intervening environment to the sensor. The information is usually carried via electromagnetic radiation in the visible, infrared, or microwave bands. Remote sensing can be further decomposed into two categories, active remote sensing and passive remote sensing. Active remote sensing is where radiation is emitted from the sensor and then reflected off of the object back to the sensor. In some systems the emitter and the sensor are not co-located, but usually they are. The reflected radiation provides information about the object. Some examples of active remote sensor types are RADAR and LIDAR. RADAR and LIDAR emit radio waves and lasers, respectively, towards the target. The difference in the timing between the emitted and returned radiation, allows the position of the object to be determined within some error bounds.

Passive remote sensing is where the radiation is emitted by the object itself or the radiation is emitted by another source, like the sun, and reflected off the object. Some examples of passive remote sensing are visible and infrared cameras. The wavelengths which are in these bands of light can be seen in figure 3-1. A visible sensor can detect light in the visible range which was emitted by the sun and reflected by the object. In the case of a fire, the visible light could be emitted by the object of interest, see

figure 2-2 . Similarly, an infrared sensor can detect light , in the infrared range which could either be emitted by the sun then reflected by the object, or heat emitted by the object itself. Some common uses of remote sensing, are military surveillance, agricultural mapping, meteorology, resource mapping, and environmental monitoring. Photons coming off of the target need to pass through the atmosphere before they can be detected by the sensor. During this travel, certain wavelengths of light are absorbed or at least attenuated by the atmosphere. The wavelengths of light which can pass through the atmosphere with minimal absorption are referred to as windows.

Both active and passive remote sensing require that the data collected be mapped to a geographic location. To accomplish this more remote sensing systems come equipped with a GPS receiver and an inertial measurement unit (IMU) to determine the position and pointing of the sensor and the location and view angle of the target or source. With the position and heading, as well as the sensor pointing angle, the location of the image can be determined.

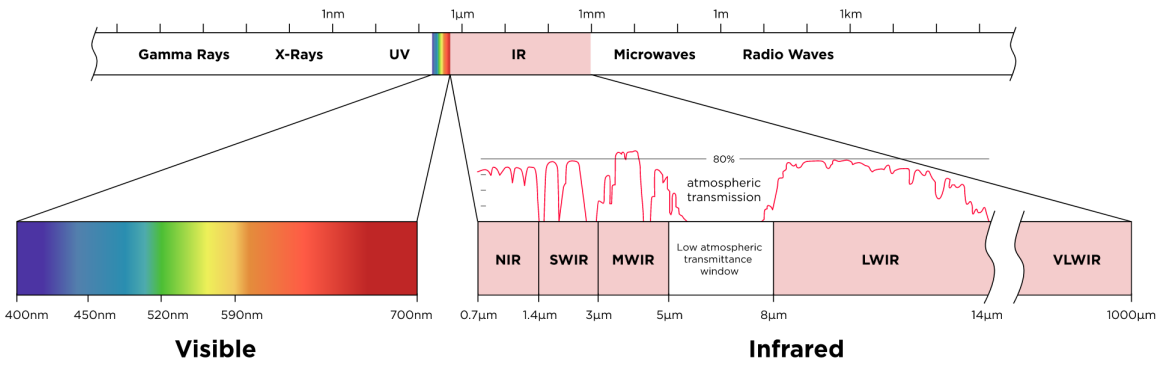

Figure 3-1: Light Spectrum and Atmospheric Transmittance [17]

3.1 Focal Plane Arrays

Focal plane arrays are arrays of light detecting elements similar to what is shown in figure 3-2. When light of a specific wavelength hits one of the detecting elements, a photon is transformed into an electron which creates an electric charge and ultimately a voltage that can be read precisely. The wavelength which the detecting element is

sensitive to depends on the material of the detecting element and the filter placed in front of it. A sensor which is capable of capturing light from multiple wavelengths is referred to as a multi-spectral sensor. This can be done by placing different types of filters over the detecting element for each desired wavelength. For example, silicon photodiodes are sensitive to light from 0.2 to 1.2 μm [11]. Then applying a filter which only allows light of 0.65 μm to pass through will result in the detector only detecting the color red. The amount of voltage for detectors in the visible and infrared range depends on the number of photons which hit the detecting elements. While a larger pixel size will generate a higher signal strength from a larger number of photons hitting the detecting element, a larger pixel also has a larger projection on the object meaning it has a lower resolution. The detecting elements in the array can be arranged in one of two different methods CMOS or CCD. CMOS arrays are made up of an array of individual pixels as opposed to CCDs which are a monolithic silicon with an electrical grid masking to divide the structure into separate electrical potential wells. CCDs have been around for a long time and can be made into large arrays like 5k x 5k, corresponding to 25 megapixels. CCDs can also be made very small for use in small electronics, like cell phone cameras. Advances in CMOS technology arrays, have made them virtually equivalent to CCDs such that they have been incorporated into many modern day electronics. Bit depth has to do with the readout electronics behind the arrays, and is the number of bits used to digitize the electrical signal (typically 12 or 16 bits nowadays). This digitization is matched to the readout noise of the system and the total well capacity. The center to center distance between two pixels is the pixel pitch of the array. The smaller the pixel pitch, the more pixels can fit on a given detector. Additionally, a smaller pixel pitch allows for a lower viewing distance, which for remote sensing means a lower effective focal length. One downside of a smaller pixel pitch is that it has a smaller well capacity and therefore you can't take as long of an exposure. Alternatively, having many large pixels would result in a more expensive system, since the optics would need to be much larger. Pixel pitch and array size are two of the primary inputs into the model used to characterize the candidate imaging systems. This is an important issue for fire detection as the precise

location of a fire needs to be pin-pointed to mount an effective response.

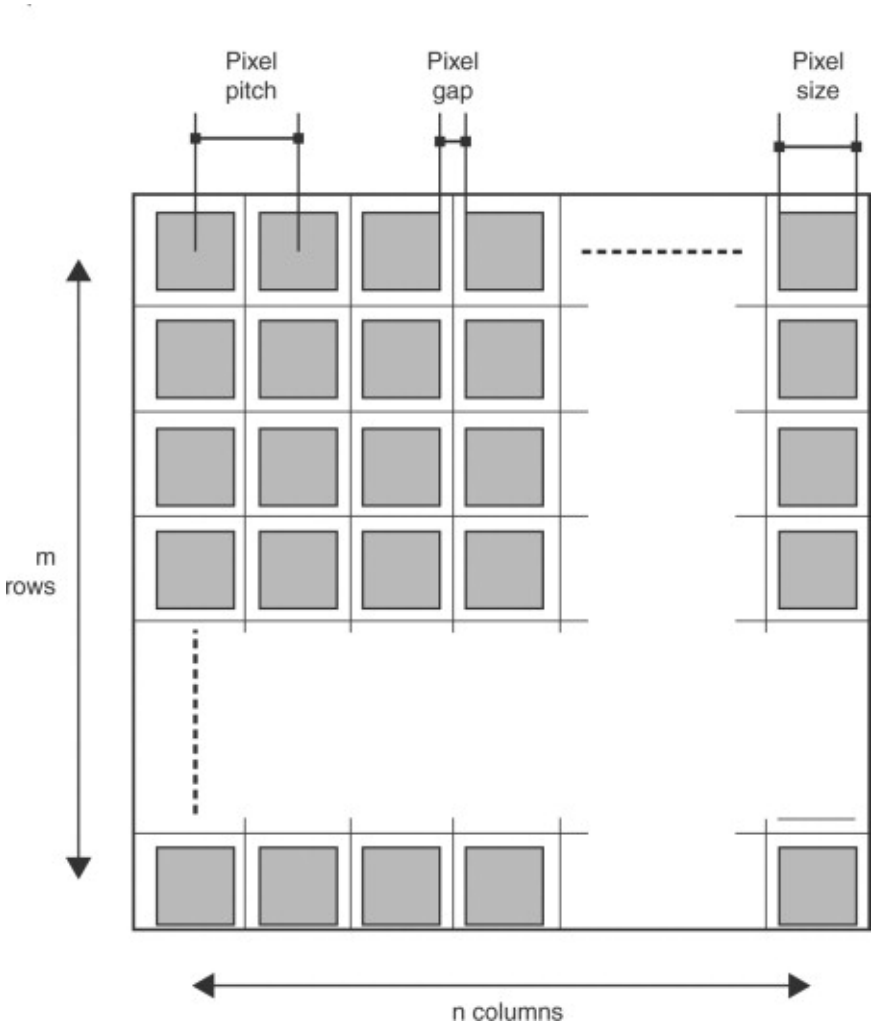

Figure 3-2: Focal plane array example [60]

Visible

The least expensive detecting elements used for remote sensing are those that detect light in the visible spectrum which goes from 400 to 700 nanometers. For any detector, there are specific ranges which the detector is more sensitive to than others. Some sensors are only sensitive to a few wavelength ranges in the visible spectrum, like RGB cameras, due to filters being placed over the detectors. Combining the data from visible light sensors can create true color imagery. This type of imagery can more easily communicate information to humans, who are primed to information in

this format.

Infrared

Infrared light ranges from over 0.7 μm to 14 μm wavelengths. Infrared is often further broken down into smaller sub-bands, as defined in table 3.1.

Band	Abbreviation	Range (nm)	Uses
Near Infrared	NIR	750-1400	Water Absorption. Reflected light
Short-wave infrared	SWIR	1400- 3000	Water Absorption. Reflected Light
Mid-Wave infrared	MWIR	3000- 8000	Detecting heat. Emitted light.
Long-Wave infrared	LWIR	8000 - 14000	Detecting heat. Emitted Light

Table 3.1: Infrared Bands

Light in the NIR and SWIR bands normally is reflected off of objects and can be used to determine the amount of water absorption of an object. For this reason they are often used in vegetation indices. An additional benefit of light reflected through these wavelengths is that they can penetrate through certain things, like smoke, which would otherwise obscure the visible spectrum as seen in figure 3-3. The MWIR and LWIR bands detect heat emitted from a source. Sensors that detect light in the IR bands usually require active cooling so that the detecting element can maintain a thermal difference from the desired heat source and reduce the input. There is a class of detectors that use micro bolometers which work in the LWIR band (8 to 14 μm) and don't require active cooling. This comes at the cost of reduced sensitivity compared to cooled detectors [2]. For remote sensing at large distances, higher sensitivity would be preferred, since the number photons reaching the sensor would be less than if the sensor were close to the target. The peak wavelength at which a certain temperature can be observed at can be determined using the Wien's displacement law where λ_{max} is the maximum wavelength, Temperature is the blackbody temperature, and b is the

constant of proportionality.

$$\lambda_{max} = \frac{b}{Temperature} \tag{3.1}$$

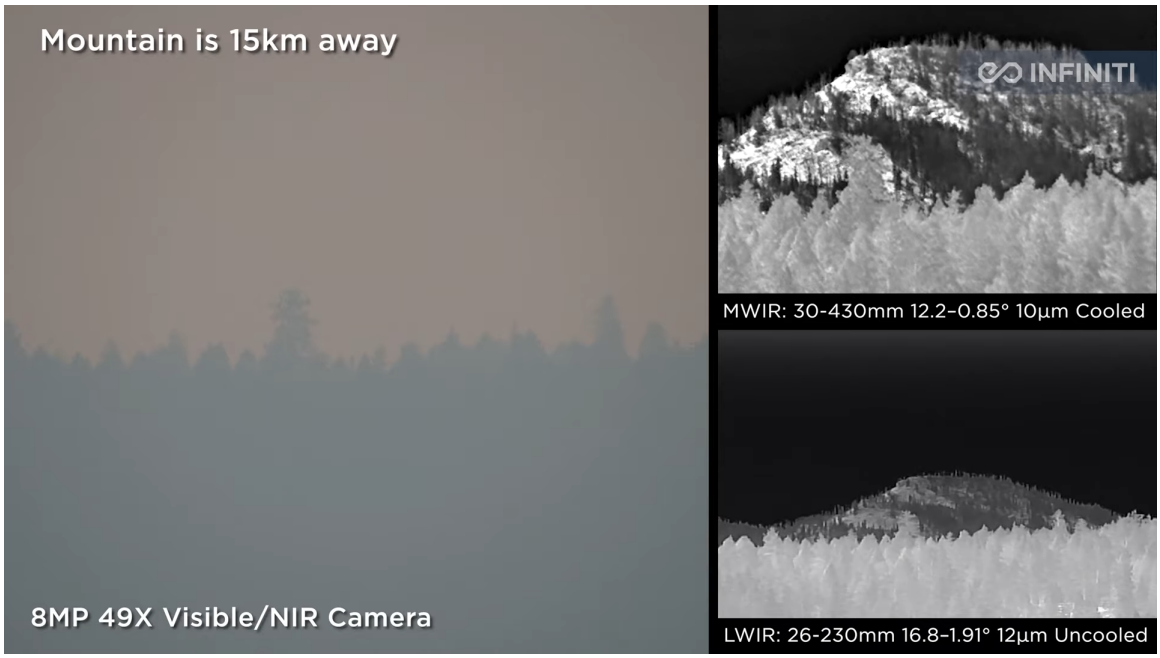

Figure 3-3: Visible, MWIR and LWIR looking through fog [35]

3.2 Optics

Telescopes are a standard component used to enhance detection. An example can be seen in figure 3-4. Telescopes are categorized based on whether they are using reflecting optics, or refracting optics or combinations of both. Within the tube of the telescope, the first optical element that the light hits when entering the telescope is known as the primary (mirror). The diameter of this element is the aperture of the telescope. The larger the aperture, the more light can enter the telescope per unit time. The distance that the light travels from the primary to the image plane is called the focal length.

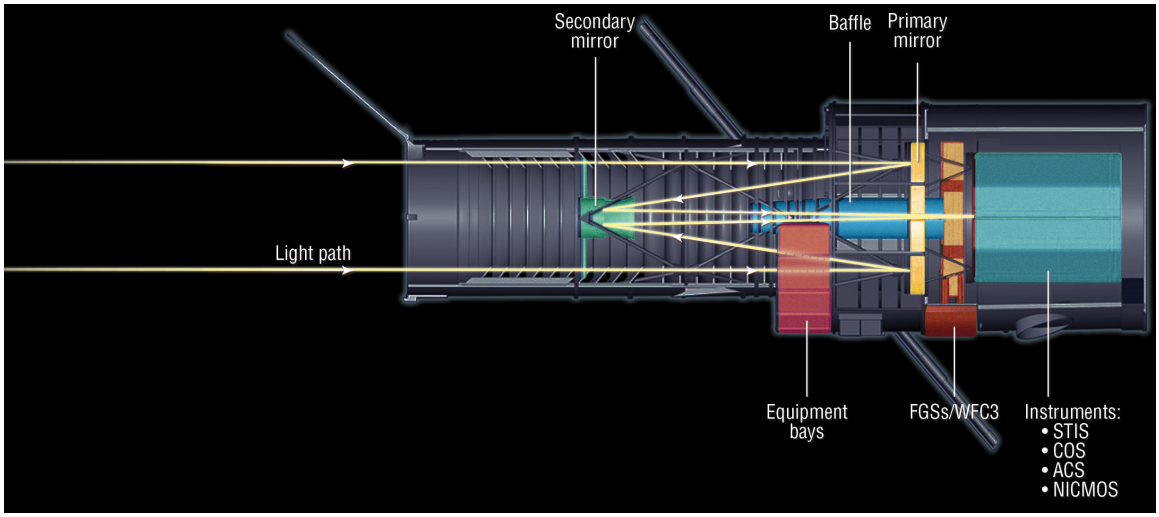

Figure 3-4: Cassegrain Telescope Optics of the Hubble Space Telescope (HST) [39]

Since the magnification of the image is the ratio of the apparent size of the image to its true size, the larger the focal length, the greater the magnification. Another important ratio of the optics is the f-number, which is the ratio of the focal length to the diameter. The f-number is also referred to as the speed of the optics, which is related to how curved a surface can be. The ground sample distance (GSD) is the area which one pixel projects on the ground, as shown in figure 3-5. The GSD is a key input for our fire detection model since it is directly related to cost and size of the optical package. The instantaneous field of view (IFOV) is the ratio of the pixel pitch to the focal length, as seen in figure 3-6.

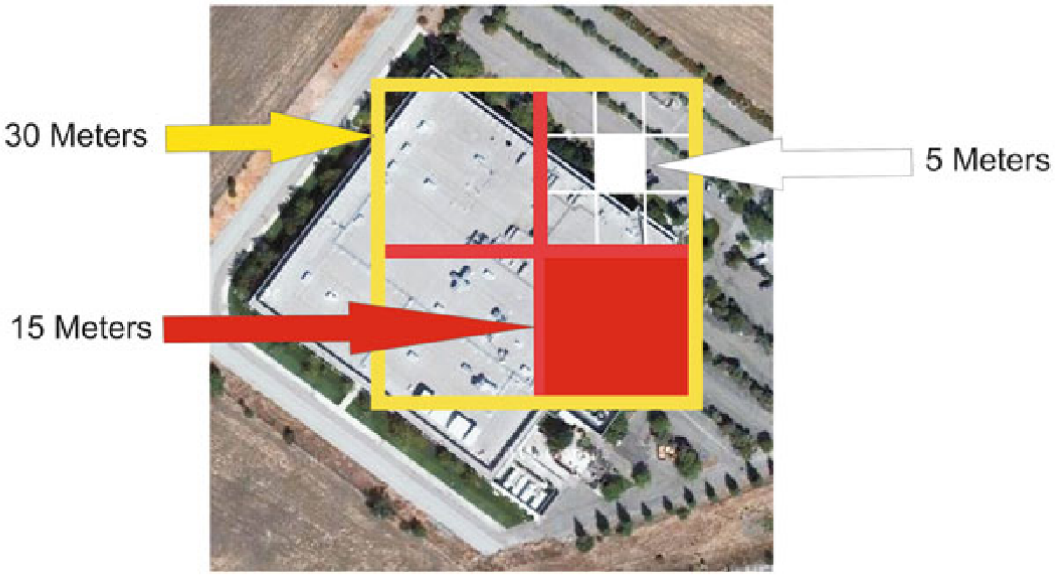

Figure 3-5: Ground Sample Distance [44]

The angular resolution is the smallest angle at which you can differentiate two objects. The "resolution" of the instrument is defined by the Rayleigh criteria in equation 3.2. If the sensor is meant to resolve an object on the ground, multiple pixels across the object are needed. If the sensor is just meant to detect the presence of the object, it can theoretically be done with a single pixel. However, oversampling or at least Nyquist sampling (two pixels per point source) is usually desirable.

$$Diameter = 1.22 * lamda/resolution \tag{3.2}$$

Since the focal plane has many pixels in an array, the total field of view (FOV) is the IFOV multiplied by the number of pixels in the crosstrack direction (for a push broom sensor). The swath width or the width of the projection of all the pixels in the crosstrack direction of the focal plane can be found by multiplying the FOV by the distance to the ground. Here we will see large differences between sensors mounted on towers, on aircraft, and on satellites.

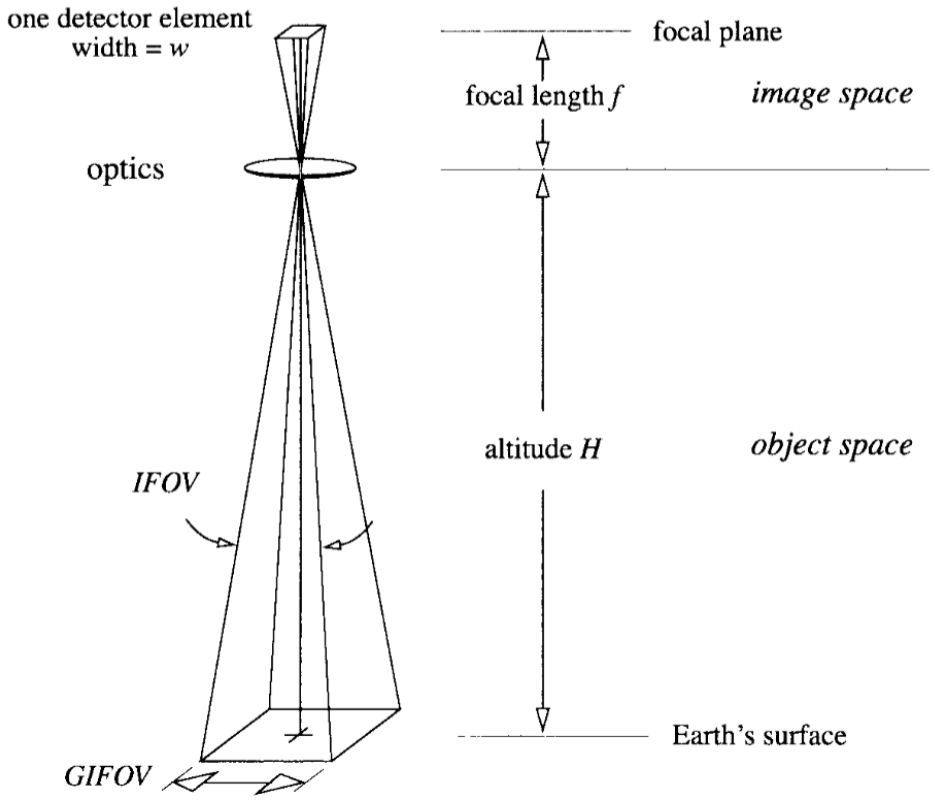

Figure 3-6: Instantaneous Field of View [56]

3.3 Sensor Systems

Airborne Systems

Airborne remote sensing is one of the more accessible forms of remote sensing, especially with personal drone technology becoming more prevalent. Low flying personal rotorcraft drones run the risk of getting hit with the fire suppression slurry deployed by fire fighting aircraft tankers and have a small swath width. For this reason most remote sensing aircraft fly at higher altitudes. Airborne remote sensing has a relatively high operational cost, due to the need to burn fuel to stay aloft. Some aircraft are on loan from the US military, like the C-130 or the Cobra helicopter. Often airborne sensor systems are gimballed on a turret, as shown in figure 3-7, which allows the whole sensor to be rotated such that it can scan an area larger than if the sensor were just pointed at nadir (straight down). One way to do this with a focal plane

array is to move the sensor side to side in a whiskbroom pattern. The tradeoff of moving the sensor in this manner is that as the sensor points further away from nadir, and the distance to the target increases which increases the GSD resulting in a lower quality image. Conversely, a pushbroom sensor scans the area with the movement of the platform (without rotating the sensor). This method either requires a wider array with more cross track pixels, or multiple passes of an aircraft.

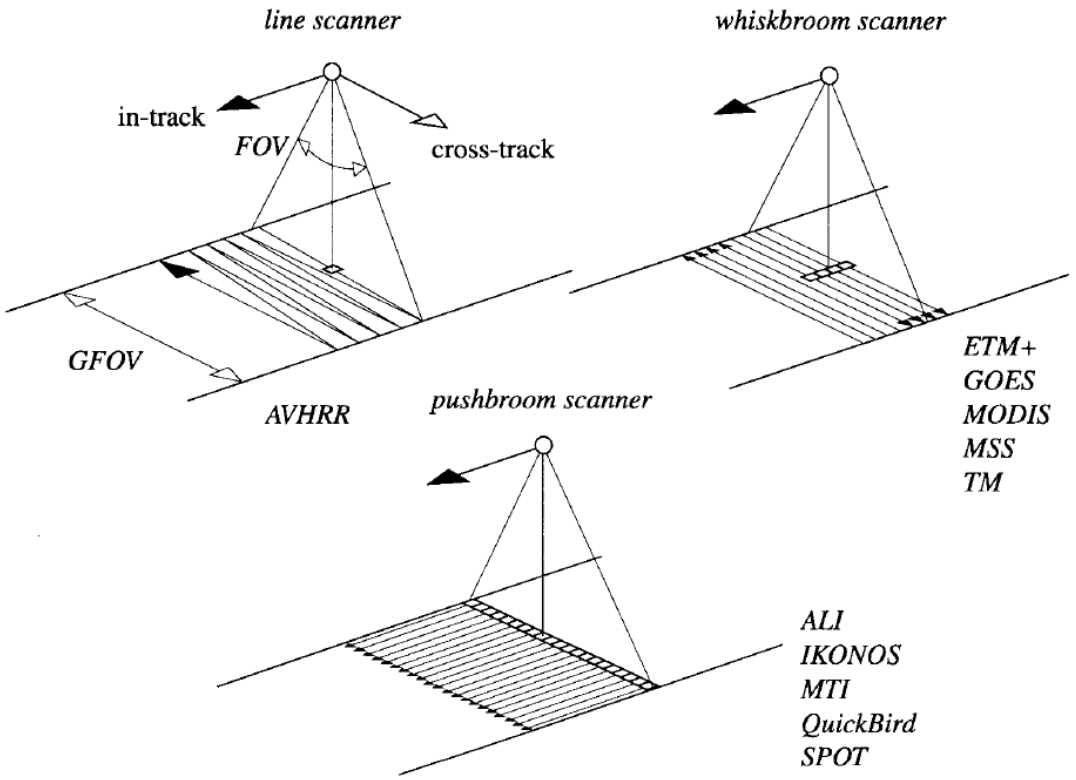

Figure 3-7: Gimballed Sensor Systems and their Ground Tracks for different Instruments [56]

Spaceborne Systems

As opposed to airborne systems, spaceborne systems don't need to constantly burn fuel to stay in the use environment. Space systems are able to change their pointing angles, similar to airborne gimballed systems, but this is often done by changing the angle of the elements inside the telescope as opposed to the telescope itself. Additionally spaceborne systems, due to their altitude, have a much higher swath

width. The tradeoffs are the high launch cost, increased engineering costs (due to existing in a vacuum with temperature extremes), and larger GSD for comparable optics of an airborne system. Spaceborne systems, are also limited to a fixed orbital path, unless they spend fuel to reconfigure their orbit [52]. For geostationary systems this means that the period of orbit is equal to the period of Earth's rotation, so the satellite is always in the same relative position to a ground target. In order to get to a geostationary orbit the system needs to get to nearly 36,000 km above the Earth's equator. Low Earth orbit (LEO) satellites, which orbit at altitudes of 2000 km or less have a higher spatial resolution for the same optics compared to a geostationary system. In figure 3-8 we can see four different systems, each equipped with the same sensor. It can be seen that the swath changes size depending on the distance from the target. Systems other than geostationary orbit systems orbit asynchronously with the orbit of the Earth. A satellite at an equatorial orbit can view the same area every orbit, but if the target area is at a higher latitude the satellite needs an inclined orbit. An orbit which is inclined enough that it passes over the Earth's poles is referred to as a polar orbit. When at an inclined orbit, since the Earth is also rotating, when the satellite completes an orbit, it won't be looking at the same area it was during the start. The lower the altitude of the orbit, the shorter the orbital period of the satellite. So a lower altitude orbital satellite would have less time to view a given area and have to wait until it synchronizes with that area again. A satellite can also be put into a more eccentric orbit where the orbit is more elliptical rather than circular. This would cause the satellite to move faster during one portion of the orbit and slower in the other. This allows a satellite to point at a target for longer during the slower portion of the orbit, but during the slower part of the orbit the satellite would be further from the earth's surface resulting in lower image quality.

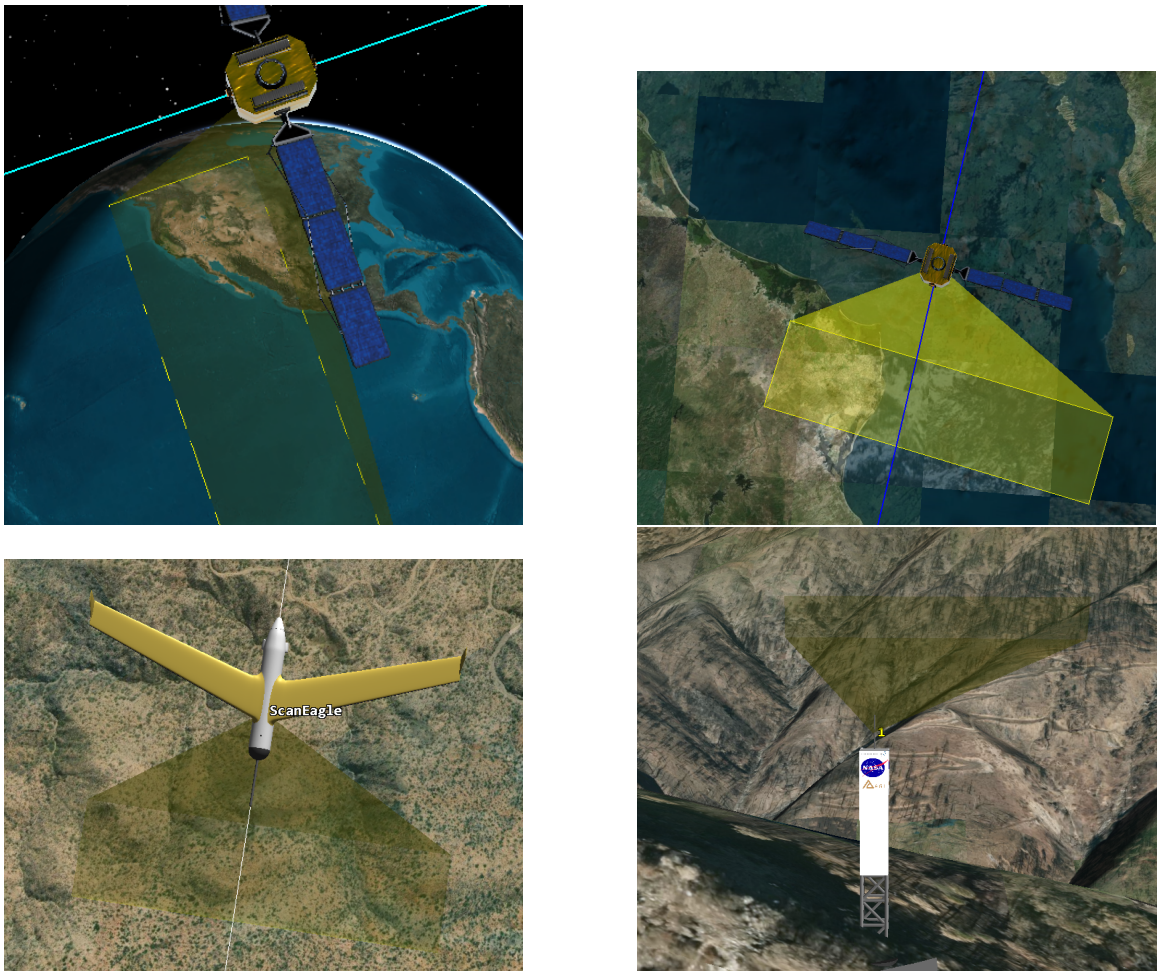

Figure 3-8: Remote Sensing Platform Examples: GEO Satellite (Top Left), LEO (Top Right), UAV (Bottom Left), Fire Tower (Bottom Right)

The LandSat 8 and Sentinel 2 satellites are often used for fire related remote sensing. The LandSat satellite orbits in a nearly polar orbit at about 705 km altitude [6]. Sentinel 2 is also at nearly a polar orbit and about 785 km altitude [9]. Both satellites have a large number of days between revisit to a given area (typically up to 16 days depending on latitude of the target). Other satellites used for fire science like MODIS or Suomi NPP which is carrying the Visible Infrared Imaging Radiometer Suite (VIIRS) also has a long repeat cycle. A higher repeat cycle or revisit time mean that it would not be useful for time sensitive remote sensing like fire detection.

Name	Inclination (deg)	Altitude (km)	Repeat Cycle (days)
LandSat 8 [6]	98.22	705	16
Sentinel 2 [9]	98.62	786	10

Table 3.2: Satellites Commonly used for Fire Science

3.4 Ground Stations

After the data is collected by the sensor it needs to be downlinked to a ground station so that it can be used by personnel on the ground. This requires a transmitter on the sensor or platform which transmits at a single frequency. The power of this transmitter is measured using the equivalent isotropic radiated power (EIRP). On the way to the ground there are multiple ways in which the signal power is attenuated. The amount of loss that occurs as the signal moves through free space is referred to as free space path loss (FSPL) and can be calculated using the equation below where d is the distance between the antennas, f is the signal frequency, and c is the speed of light. This is the logarithmic form of the space loss equation.

$$FSPL = 20 * log(d) * 20 * log(f) * 20 * log(4 * pi/c) \tag{3.3}$$

Additionally, there is signal loss that occurs from travelling through the atmosphere that depends on the frequency of the signal.

Once the signal reaches the ground, a parabolic satellite dish can be used to focus the incoming signal to a receiver. This setup requires a motor to follow the position of the sensor as it moves. A more modern technique is to use electronically steerable antennas (ESA) which in addition to significantly reducing the wear of the antenna increases the accuracy and speed of the antenna's beams. Each receiving antenna has a maximum scan angle which it can track the sensor. The receiver on the antenna has a given bandwidth which constrains how much information it can intake. Another important parameter is the ratio of the peak gain, where the boresights of

the antennas are aligned, to the noise generated by the ambient temperature at the antenna. The ratio of the signal strength to the sum of all of the losses is referred to the signal to noise ratio (SNR). With the SNR known, the spectral efficiency (SE) can be determined using modulation and coding (MODCOD). The throughput can then be found by multiplying the spectral efficiency by the usable channel bandwidth of the receiver. The throughput is the rate at which data can be downlinked to the ground station from the sensor. [22] The ground station could be at fixed location which distributes the information to the users as seen in figure 3-9. If the ground equipment size, weight and power (SWAP) allows it, the ground station can be mobile. In the case of wildland fires, the faster the data can become available, the more up to date information can be available to fire management. Additionally, more recently available data would allow for wildland fires to be discovered closer to the time of their ignition.

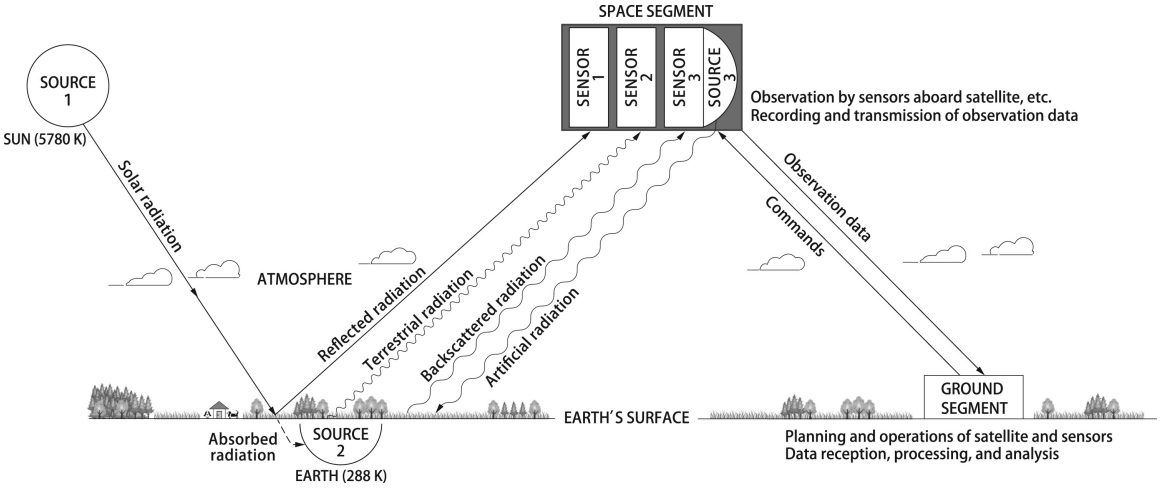

Figure 3-9: Ground Segment [41]

3.5 System of Systems

There are obvious tradeoffs for different kinds of sensor systems. Airborne systems are closer to the ground so smaller optics can be used than spaceborne systems to get the same ground sample distance. Spaceborne systems on the other hand, due to their larger distance to the target can have a much larger swath width with the same

field of view as an airborne system. The platforms themselves have various trade-offs as well. An aircraft requires fuel or electrical energy for each image collection mission. While a satellite doesn't need fuel for each image collection mission, but it requires a tremendous amount of fuel to get to orbit. Given that there are different needs for the different functions of remote sensing in wildfire management, there may be value in using different combinations of systems. Combining multiple complex systems together to create a new larger system which provides additional functionality or performance is what is referred to as a systems of systems. According to the International Council on Systems Engineering (INCOSE) Systems Engineering book of knowledge (SEBOK) there are 4 different types of system of systems: Directed, Acknowledged, Collaborative, Virtual [13]. In a directed SoS, even though the component systems can operate independently, the components normally function hierarchically under the top level SoS. In an acknowledged system, even though there is an understood combined function, the systems are not created, designed, or funded under the same hierarchy. In a collaborative SoS, the combined operation is done voluntarily by each of the component systems. In a virtual SoS, the new functionality emerges organically and there is normally no central hierarchy. At the moment the remote sensing activities are structured as a collaborative system of systems, where various organizations like NASA, USGS, CalFire, various levels of government, and various branches of the military work together (along with their resources) to provide remote sensing capabilities. There are many reasons why structuring the system of systems like this is not optimal. If more of a specific resource type is needed, the request needs to go through a different organization's acquisition process. The organization which owns the resource may not see the SoS use case, as the primary use of the component system. When the owner has already allocated the resource to a function which it deems higher priority, contention for that resource arises and the requester may not be satisfied. Other difficulties could arise if the owner modifies the resource such that it no longer satisfies the requestor's needs. These difficulties could be prevented by having a directed SoS whose main purpose is to support fire management use cases. While this would have a higher upfront cost and maintenance

costs than borrowing systems, it could provide higher utility to the fire management SoS which would result in a SoS that is more stable over time.

The main question in this thesis is what combination of vehicles and sensors would form an "optimal" system of systems, specifically for fire detection and management.

Chapter 4

Methods

4.1 Tradespace Analysis

When engineering a complex system, there are many decision factors of the system which contribute to key attributes or capabilities of the system. Each of these factors could have different levels of significance to different stakeholders. Often these decision factors are in tension, such that investing in one will decrease the other. Trade studies can be done to analyze the different system architectures on a level playing field. The bounded area on which the different architectures are compared is referred to as the tradespace. From analyzing this tradespace, we can eliminate candidates which are not viable as well as determine what the best options are for different circumstances. The normal sequence of conducting a tradespace analysis is as follows [34].

4.1.1 Understand the Problem statement

The problem statement is a short description of an undesirable condition which doesn't include extra information that may bias the reader towards certain solutions. For this study the problem statement is that, firefighting personnel need a better way to predict, detect, monitor and assess the damage from wildfires because every year, the damage from wildfires increases.

4.1.2 Identify Stakeholders

Understanding who all will benefit from the system and who will be affected by the system is important to understanding the needs of all the different groups. Stakeholders can be further broken down into three groups, Charitable beneficiaries, beneficial stakeholders, and problem stakeholders [36]. Charitable beneficiaries don't provide anything to the system, but benefit from it performing well. Beneficial stakeholders provide resources to the system and benefit from it performing well. Problem stakeholders don't necessarily benefit from the system performing well. Some of the stakeholders for the system proposed in this study can be found in table 4.1. Interview and Panel results from interactions with potential stakeholders can be found in section 5.1

Charitable Beneficiaries	Beneficial Stakeholders	Problem Stakeholders
General Public	Firefighters	Airports
Insurance Companies	Fire Science Community	Space Launch Companies
Local Wildlife	Government	FAA

Table 4.1: Stakeholders

4.1.3 Identify and Weight Decision Factors

Identify which decision factors would be necessary to determine the utility of a design and allocate weights to them based on importance to the stakeholders. Four functions have been identified for this study, fire prediction, fire detection, active fire monitoring, and fire damage assessment. Since improvements in utility for each of these functions (that we will call "design factors") could potentially save lives, they are all weighted equally. The ideal system would perform well in each of the fire management phases denoted by these design factors.

4.1.4 Identify and Weight Decision Factor Criteria

For each of the design factors identify what criteria would be used to judge its utility and weight those criteria based on the stakeholders importance. The decision factor criteria with their associated weights are denoted in tables 6.6 and 6.7.

4.1.5 Characterize Utility Functions

Use the design factors, their criteria, and associated weights to create utility functions. A utility function is a function used to determine the value which a candidate architecture would have to the system stakeholders. This function can be linear or non linear, and should include the system's associated design factors. The utility function for this study is described in section 6.4.5.

4.1.6 Identify Viable Candidate Solutions

Identify candidate solutions and remove any candidates which don't comply with the design requirements or are infeasible. Infeasible candidates are removed in the model as described in section 6.4.

4.1.7 Evaluate Candidate Solution Decision Criteria

Run the viable candidate solutions through the utility functions and evaluate the resulting utilities. Analysis of the candidates output by the model is done in chapter 7.

4.2 Utility vs Cost

With the utility of the candidate designs determined, one of the more useful graphs to help determine the optimal solutions is the Utility vs Cost graph, as seen in figure 4-1. On this graph, the Pareto frontier is a curve comprised of points on the graph where there is no other point that could be better in an aspect without getting worse in another aspect. This curve allows multiple optimal designs to be gathered for

different costs or performance needs. The Pareto frontier graphs for this study are documented in chapter 7. Each point in the tradespace will represent a different system of systems architecture of sensor systems for wildfire management.

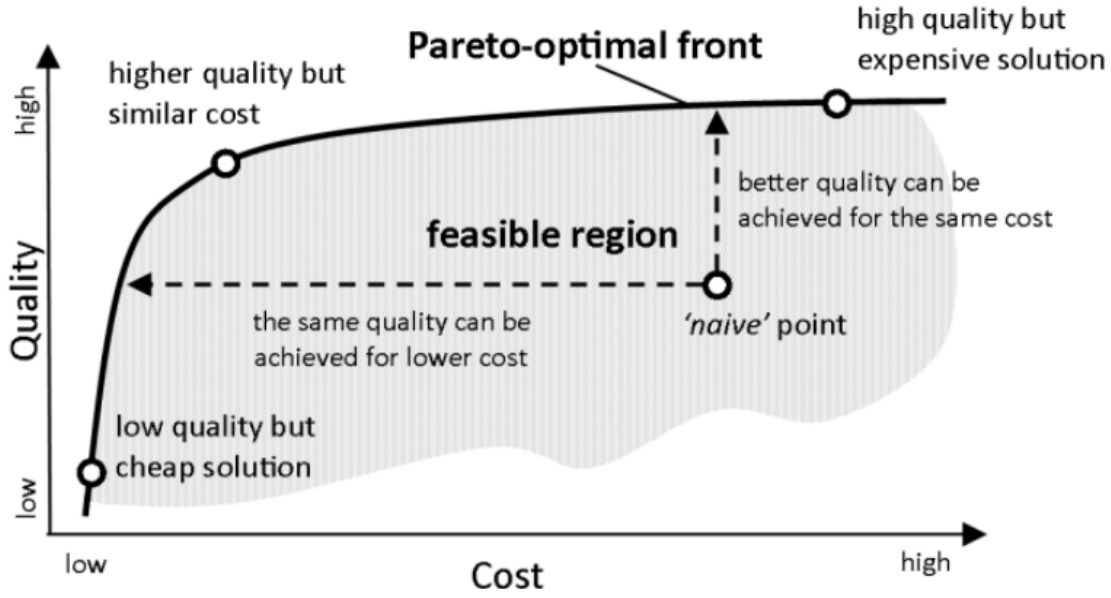

Figure 4-1: Generic Tradespace with Pareto Frontier [30]

Chapter 5

Stakeholder Needs

5.1 Interviews

5.1.1 United States Geological Survey

The United States Geological Survey (USGS) is a U.S. government scientific agency which studies earth science including natural hazards, like wildfires. One of their specialties is remote sensing, which they use for resource mapping and hazard analysis. Their remote sensing capabilities include the LandSat program, which is one of the best known remote sensing satellite programs. An interview was conducted with a USGS physical scientist who specialized in wildfire management with expertise in assessment and prediction of wildfires. Fuel mapping was discussed, including the LandFire fuel mapping project. When the LandFire project was started in 2002, there was no consistent nationwide dataset available for fuels. The resolutions for wildfire management depends on the application. For the LandFire project 30m spatial resolution was selected since it would be high resolution enough to provide functional information, but low resolution enough that it could be used at a large level. The LandFire project only updates their maps once every couple of years, but are looking to transition to an annual update cycle. The fuel data, the weather, and terrain are all inputs into the Wildland Fire Decision Support System (WFDSS). WFDSS is a web-based tool to help federal and state fire management personnel

with near term, short term, and long term wildfire related decision making. Aircraft like the C-130 and the Cobra, or the Superking Air 200 are used for monitoring the progression of the fire. These efforts take place in the night and the data is downlinked during the day. After the fire, is it imperative the understand the extent of the damage as soon as possible and prescribe treatments. To do this, the Burned Area Emergency Response Specialists (BAES) use pre fire and post fire vegetation indices to determine the damage. The data for the vegetation indices are normally collected using either Landsat or Sentinel 2 satellites. The data collected is normally available within a couple of hours. The vegetation index used to generate pre-fire risk maps is NDVI while NBR is used to analyze post fire damage. Usually, the same index is used both pre and post fire to create a differenced index, but if the data from the same index isn't available other indices can be substituted in. In the future it would be useful to have more near real time data at a higher resolution. For active fires, having more real time data is necessary. For pre-fire areas, getting clear imagery with both soil and fuel moisture would be very useful. For post fire, LIDAR and RADAR could be used to get fuel structure, as opposed to just getting the moisture through vegetation indices.

5.2 Panels

5.2.1 The Power of Real-Time Data for Firefighting

The panel "The Power of Real-Time Data for Firefighting" took place as part of the GeoInt 2019 Symposium [24]. The panels came from a range of backgrounds including co-founder of Interra (a wildfire remote sensing data distribution company) , the director of USGS, CEO of the Western Fire Chiefs Association, a data scientist for CalFire, and a Ph.D. in post fire research. One of the panelists began by discussing the Camp fire, and how significant of an effort it was to fight the fire. It was mentioned that in wildfires, the fire doesn't actually spread by active flame contact. The fire leaps ahead of the flame front via what is referred to as ember cast, where embers

move ahead of the front and create spot fires. These embers can move over a mile beyond the flame front to create spot fires. This is how the camp fire was able to move 6.3 miles in an hour and a half. Currently, wildfire incident commanders are using paper maps to plan how to combat wildfires. So, the data being gathered by remote sensing isn't being converted into information and being communicated in a way that can support those on the ground. Hurricane models, earthquakes, and other meteorological data can be viewed in real time by any lay person, but real time wildfire data takes at least 24 hours to get to the incident commander. Part of the reason why the wildfire management efforts are still so archaic is because, only recently have wildfires started to exponentially increase in the amount of damage that they cause. The old methods used in firefighting may have worked 30 years ago, but things are getting much worse. Twenty years ago there may have been hundreds of homes lost, where today a single incident can claim multiple thousands of homes. Forty billion dollars have been spent over the past two years on insurance recovery and firefighting costs relating to wildfires in the state of California alone. Currently, there are two state of the art multi-mission aircraft in Colorado that are dispatched to all major wildfires. These aircraft are equipped with EOIR sensors, on-board image processing which can downlink the imagery and is made available to firefighters within 10 minutes. Firefighters need this information in the form of shape files so that they can see where they are in relation to the fire line. In the future they would like to have higher resolution fuel models that use data from both hyperspectral and LIDAR sensors. They would also need real time data, which they define as persistent fire perimeters at $1m^2$ resolution with 2 minutes or less latency before it is a shape-file. To get to the low latency AI will likely been needed. One of the panelists discussed how fuels can change over time. For example, if sage brush is burned away it could be replaced with cheat grass that could grow in its place. Cheat grass is extremely incendiary, so the potential fire dynamics of this area change dramatically. Knowing this information would allow for more accurate fire prediction. There was no discussion of fusing data from airborne or spaceborne remote sensing with ground based remote sensing.

A more accurate fire prediction would allow for assets to be better pre-positioned to deal with potential fires. The landfire program is not real time, but could capture this change. The landfire project is also mapping the U.S. with LIDAR to get high precision digital topography and density of the forest canopy. The USGS also has a product that maps hot spots in the United States every four to six hours that is disseminated to wildfire incident commanders. The USGS also has a separate tool to show the post fire likelihood of debris flow.

5.2.2 Hot Mess: Remote Sensing Applications for Wildfires and Other Natural Disasters

"Hot Mess: Remote Sensing Applications for Wildfires and Other Natural Disasters" was part of the Geodistancing Live Webinars by L3Harris which occurred in May 2021 [43]. The two panelists were remote sensing specialists, one coming from San Diego State University one coming from L3Harris. Both the hosts as well as the guests specialize in remote sensing for wildfire management. The panelists discussed what can be done to mitigate the occurrence of fires and the roles of different remote sensing technologies. Multispectral and Hyperspectral imaging can be used to analyze tree species and their relation to fires. LIDAR and SAR can be used to analyze biomass, or the quantity of fuel in a given area. One of the panelists suggested that fires starting in certain unexpected locations may be due to not having an appropriate knowledge of the biomass fuel prior to a fire. One of the panelists mentioned a company called *Range and Bearing*, which used thermal sensors on a plane that can see through smoke and provide information to the ground within minutes. This information can support the firefighting activities by providing detailed location to tankers or letting the ground crew know where they are in relation to the fire. Additionally, fires can occur in very steep areas, specifically in Colorado. After a fire, when the snow melts, the run off can destabilize the soil if there is enough damage to the forest resulting in landslides and floods. Remote sensing can be used to determine the damage by using a burn severity index [58]. If this information is then merged with information about

the terrain, the location affected the most post fire can be discovered. In recent years, there has been more recent data available as well as new forms of data coming from LIDAR and SAR sensors. Having these new modalities, as well as having previous modalities more frequently, has been a boon to the field of wildfire management. In the future the hope is to use remote sensing to help monitor the incursion of invasive plant species that may increase the likelihood of wildfire. For example, invasive grasses may catch faster than the native grasses resulting in a faster fire spread. Another desire is to have real time remote sensing data that can tell the exact location and temperature of the fire. Communicating this real time information from the active fire front to the firefighting command structure and the active firefighters would greatly increase the effectiveness and the safety of the firefighting efforts. One of the panelists suggested that this could be done with an airborne sensor at a lower altitude. This sensor would need to have both visible and infrared bands (NIR, SWIR, and LWIR). The airborne sensor would have to fly at an altitude above the tanker aircraft or they would risk getting destroyed by the dropped slurry. When questioned on drones, there was concern regarding the ability to downlink the amount of data that would be generated. Additionally, the benefit of having a larger field of view image was discussed, especially for larger fires. These larger field of view images would typically come from satellites due to their high altitude, and would allow a person to see the whole scope of the fire. But, this would result in lower resolution imagery than a lower altitude sensor. There was no mention of high altitude non-spaceborne platforms, like High Altitude Platfom Systems (HAPS), which (at 60-70 kft) would be between normal aircraft altitude and low earth orbit satellites. So, one of the panelists mentioned the benefits of having multiple different remote sensing platforms to maximize the benefits of each while minimizing the tradeoffs. The one tradeoff from this method though is that it would generate an extremely large amount of data that would have to be fused in near real-time. Ten platforms, each equipped with the same sensors as the LandSat8 multispectral satellite, would generate close to 10 terabytes worth of data per day [7]. Also, the availability of multiple sensors at multiple altitudes to monitor a wildfire would be more costly than just having a

single dedicated sensor available.

Chapter 6

Model

6.1 Design Constraints and Assumptions

The fire management system of systems model developed here does not include any active remote sensing calculations. LIDAR and SAR remote sensing are comparatively new modalities and there aren't as many theoretical models to use for design estimation. The cost models that do exist for airborne EOIR sensors were made using a very small sample set, and come from primarily military sensors. No existing models were found for the weight of EOIR sensors, which is an input into other cost models. No cost model for the ground station could be found, so the cost was estimated at 50K USD per ground station. Each of these ground stations were also assumed to be using the Ku band to communicate with the sensor. It is assumed that the sensors are operating in a pushbroom mode. This is done to reduce the complexity of the model. When sensing in a pushbroom mode at nadir, the model is presenting the highest resolution case for a sensor, even if it is gimballed. This is because a gimballed sensor, not positioned at nadir, would have a larger distance from sensor to target. It is also assumed that the sensor is using a framing array focal plane to get snapshots of the target area, as opposed to line arrays. Similarly, it is assumed that a square framing array is used, so there are the same number of along track pixels as cross track pixels. The sensor is assumed to downlink the data it collects in real time. Alternatively, the system could store the data to downlink at a later time, or

use intersatellite links to downlink the data. Neither of these are incorporated in this model.

6.2 Input Parameters

All of the different detecting elements have the same wavelengths to which they are sensitive. For this model, we are initially looking at 1.7 x 10^{-6} m wavelength which is in the SWIR band. The model also uses a fixed value of 16 for the bit depth of the detecting element to match what is used on Landsat 8 [6].

Wavelength (μm)	Bit Depth
1.7	16

We will also look at other wavelengths of light in the visible, MWIR and LWIR wavelength ranges.

Wavelength (μm)	Name
0.65	Red
3.5	MWIR
10.6	LWIR

The model uses fixed costs for ground station cost, airborne system operational cost, aircraft turn around time, Mean time between overhaul (MTBO), and overhaul time (OT). The airborne operating cost is approximately the cost of the cost per hour for operating existing infrared mapping aircraft [25].

Ground Station Cost (USD)	Airborne Operational Cost (USD/hr)	Aircraft Turnaround Time (hr)	MTBO (flight hrs)	Overhaul Time (hrs)
50,000	1,000	90	100	24

To estimate the cost of the ground station operations, the cost of personnel are needed as well as the number of personnel and the software lines of code (SLOC) for the systems. The input values can be determined from the typical SLOC and annual salary [61]. The personnel are full time engineers (FTE) and full time technicians per ground station.

N_{FTE}	N_{Tech}	$Cost_{FTE}$ (USD/year)
2	2	200k
$Cost_{Tech}$ (USD/year)	$SLOC_{airborne}$	$SLOC_{spaceborne}$
150k	16,000	100,000

In order to determine the utility of a design, the functionality of the design is compared to real values from fires. For this model we used values from the Camp Fire in California (2018).

Detection Resolution (m)	Daily Monitoring Size (acres)	Distance to Fire (m)	Containment Time (days)
30	34,000	36,000	8

Additionally, certain values were stated to be desirable in future remote sensing systems. These values were also incorporated in the model to help determine the utility of the design.

Monitoring Resolution (m)	Monitoring Latency (s)
1	120

6.3 Input Variables

The model has four sensor design input variables. The altitude of the sensor platform in meters. For orbiting sensors it is assumed that the sensor has a circular orbit with a constant altitude. The minimum detectable distance of the sensor or the ground sample distance, in meters. The pixel pitch, which is the center to center distance between pixels on the detecting element. Finally, the number of cross track pixels in the detecting element.

Altitude (m)	GSD (m)	Pixel Pitch (m)	Crosstrack Pixels
3048	0.5	2 e-6	256
4572	1	10 e-6	512
9144	10	15 e-6	1024
200000	100	20 e-6	2048
2000000	1000		4096
35786000			

Table 6.1: Input Variables

6.3.1 Altitude

For the altitude variable the multiple variables represent very different types of sensors. Three of the altitudes represent airborne sensors. The range of airborne altitudes represent approximately the range of cruising altitudes for helicopters piston engine aircraft and turboprop aircraft. The higher three altitudes represent space-borne sensors aboard satellites. Since 90 percent of satellites operate at Low Earth Orbit (LEO), the first two are within that range. The 200 km altitude represents a very low earth orbit satellite which would have a very fast orbital period (and a short orbital lifetime). The 2,000 km altitude represents a satellite at the upper end of what could be referred to as a LEO satellite. Both of these satellites have an inclination of 45 degrees. The final altitude represents what is referred to as a Geosynchronous Orbit (GEO) satellite. This satellite would orbit at the same period as the rotation of the Earth, so the same area would be constantly in view.

6.3.2 GSD

In a recent panel at GEOINT 2019, titled "The Power of Real-Time Data for Firefighting" the value of high resolution fire imagery was discussed as a desirable feature in future remote sensing systems used in fire fighting. While monitoring active fires may require high resolution imagery, mapping fuels doesn't [14]. Some current sys-

tems which are used in wildfire remote sensing , like the Terra satellite instrument MODIS, have much lower spatial resolutions [45]. So the GSDs selected can go from 0.5 meters up to 1000 meters. While this is normally the output of the sensor design, we are using the stakeholder imagery needs as well as current system capabilities as inputs to the design of the system.

6.3.3 Pixel Pitch

The pixel pitch values used correspond to the smaller pixel pitch values available for large format IR and visible sensors.

6.3.4 Crosstrack Pixels

The cross track pixels used correspond to the larger detecting elements available from focal plane manufacturers [3] [19].

6.4 System Design

Angular resolution in radians can be found by dividing the GSD by the altitude.

$$Resolution = GSD/altitude \tag{6.1}$$

IFOV (instantaneous field of view) is found by dividing the resolution by 2 since 2 pixels are needed to resolve an object. For detecting fires, only part of a pixel may need to be illuminated by a fire in order to determine that there is a fire in the ground area captured by the pixel [31].

$$IFOV = resolution/2 \tag{6.2}$$

Aperture diameter can be found using the Rayleigh criterion in equation 3.2.

The effective focal length of the sensor can be found by dividing the pixel pitch

by the IFOV.

$$EFL = pixelpitch/IFOV \tag{6.3}$$

If it is assumed that the detecting element has the same amount of cross track pixels as it does along track pixels, the field of view of the entire detecting element can be found by multiplying the IFOV by the along track pixels

$$FOV = IFOV * alongtrackpixels \tag{6.4}$$

With the field of view, the swath width can be determined by multiplying the FOV by the altitude.

$$swathwidth = FOV * altitude \tag{6.5}$$

The velocity is determined based on sensor parameters in sections 6.4.2 and 6.4.1. The angular velocity can be calculated by dividing the velocity by the altitude. Then, the frame rate can be found by multiplying the angular velocity by the field of view.

$$framerate = \frac{velocity}{altitude} * \frac{FOV}{4} \tag{6.6}$$

The f number of the optics can be determined by dividing the effective focal length by the aperture diameter. The lower the f number, the more expensive the optics. So the model limits the designs to those with 2.5 f number or greater.

$$fnumber = \frac{EFL}{Diameter} \tag{6.7}$$

Additionally, the model places limitations on the size of the optics in the sensor. Candidates with optics with a diameter larger than 2 meters, or smaller than 1 cm, are deemed infeasible and removed from the model. There are very few large telescopes with apertures larger than 2m, and small telescopes can have diameters on the order of magnitude of one centimeter [27] [29].

6.4.1 Spaceborne Sensors

For spaceborne optics, assuming a spherical earth, the altitude of the sensor and radius of the earth can be used to find the orbital period.

$$T = 2 * pi * (altitude + Re) * \sqrt{\frac{altitude + Re}{9.81 * Re^2}}; \tag{6.8}$$

where Re is the mean radius of the Earth. The velocity of the spaceborne sensor can be determined using the altitude, radius of the earth and the orbital period

$$velocity = \frac{2 * pi * (altitude + Re)}{T} \tag{6.9}$$

The framerate of the sensor can be found by dividing the angular velocity by the FOV of the sensor.

$$framerate = \frac{velocity}{altitude * FOV/4} \tag{6.10}$$

The availability of the sensor is the fraction of the total time needed during which the system can be used. For geosynchronous satellites, since the satellite would always be pointing at the same spot on Earth, this would be the total time. For the other satellites that aren't synchronized with the Earths rotation, like LEO satellites, this would be the time the satellite is viewing the target area divided by maximum time to acquire. The time on target is the time which the spaceborne system could be imaging the target area.

$$maximumtimetoacquire = orbitalperiod * revisitorbit \tag{6.11}$$

$$timeontarget = alongtracktargetlength/velocity \tag{6.12}$$

$$availability = timeontarget/maxtimetoacquire \tag{6.13}$$

In order to determine the revisit time of the spaceborne sensor, System Toolkit (STK) was used to model the satellite trajectory for each orbit. When the satellite roughly covered the same area as the original orbit, it was considered the revisit orbit. Di-

agrams of the obits can be found in Appendix A.1. Multiplying the revisit orbit by the orbital period gives the revisit time. Since the geosynchronous orbit satellite is continually looking at the same area, its revisit orbit is zero, and therefore its revisit time is zero.

Altitude (km)	Revisit Orbit	Revisit Time (hr)
200	17	25.06
2000	12	24.42
35786	0	0

Table 6.2: Revisit Time

The cost of the sensor can be estimated through "Meinel's law" which uses the aperture to calculate the cost for large telescopes as shown in equation 6.14 [57][49] . The equation is multiplied by 3.84 to convert from 1979 dollars, from when the model was originated, to 2021 dollars.

$$cost = 3.84 * 0.37 * 10^6 * diameter^{2.58} \tag{6.14}$$

To estimate the weight of the spaceborne sensor in kg, we can look at other existing EOIR satellites. For a Cassegrain telescope, the larger the aperture diameter in meters, the larger the required optical structure. The larger a primary structure, the more mass is needed to reduce vibration.

Name	Aperture Diameter (m)	Satellite Weight (kg)
IKONOS	0.7	817
Landsat7	0.406	1973
Landsat8	0.7	2623
Quickbird2	0.6	1110
WorldView2	1.1	2800
WorldView3	1.1	2800
GeoEye	1.1	452
Sentinel-2	0.15	1142
Nigeria 2	0.31	300
Beijing-1	0.4	90
DubaiSat-2	0.42	300
Razak-1	0.45	190
Dove-2	0.09	5.8

Table 6.3: Spaceborne Sensor Aperture and Weight

A linear regression of the weight of the sensors and their respective aperture diameter provides a rough order of magnitude of the weight of a sensor, given the aperture diameter. The R^2 value of this model is 0.34. This relationship might be slightly lower since it is the weight of the entire satellite, which could have multiple sensors. The effect of this would be a slightly higher predicted weight, which should be acceptable for establishing a rough order magnitude (ROM) for launch cost per sensor.

$$weight = 1795 * diameter + 84.3 \tag{6.15}$$

With the weight of the sensor given, the non recurring cost of deploying the sensor into orbit can be calculated. The cost to deploy a satellite to LEO is 5 thousand dollars per kilogram, and the cost to deploy a sensor to geosynchronous orbit is 36 thousand dollars per kilogram [62] [42]. These numbers are generated by dividing the

launch cost of a rocket by the available payload mass. So, in reality the full launch cost would have to be paid even if the mass used is less than the total available payload. This isn't currently being factored in to the launch cost.

6.4.2 Airborne Sensors

To determine velocity, and endurance of the airborne sensors, the model uses a set of U.S. military UAS platforms to assign properties for the sensor. The UAS grouping depends on the platform velocity, nominal operating altitude, and the maximum takeoff weight. The altitude of the sensor can be uses to select an example aircraft from which the velocity of the platform and the endurance can be estimated. The MQ-9, MQ-1, and ScanEagle have all been used to monitor wildfires making them good example platforms on which to base an example airborne wildfire monitoring platform [1] [5].

Group	Altitude (m)	Aircraft	Velocity (m/s)	Endurance (hr)
5	>5487	MQ-9 Reaper	87	14
3 and 4	5487-1066	MQ-1 Predator	60	24
2	1066-366	Boeing ScanEagle	41	24
1	<366	Boeing ScanEagle	8.33	1.5

Table 6.4: UAV Platforms as a benchmark

The availability of the platform can then be calculated using the following equation, where acTAT is an estimated aircraft turn around time and the fire containment time depends of the fire inputted into the model.

$$availability = \frac{\frac{Endurance}{Endurance+acTAT} * (firecontainmenttime - TotalOverhaulTime)}{firecontainmenttime} \tag{6.16}$$

To calculate the cost of an airborne sensor, multiple cost models are used. The cost of the actual sensor can be calculated by a specific cost model made from military EOIR sensors on UAVs [46]. The inputs to the model are the resolution of the sensor

in microradians, whether the sensor has tracking capabilities, and when the sensor was used on its respective platform.

$$cost = 1e3 * (290.18e6 * resolution^{-0.830} * e^{1.829*trk} * e^{-0.169*(FY-1900)} \tag{6.17}$$

The resolution was previously calculated, none of these sensors have tracking capabilities and 2021 was used as the first year.

The cost of the platform that carries the sensor can then be calculated using a separate model [59]. The model's only input is payload, and the model was constructed using only seven platforms.

$$platformcost = payload * 8000 * 2.2 \tag{6.18}$$

Since the sensor has not yet been designed, the payload weight of the sensor needs to be estimated. A simple method to estimate the payload of an airborne EOIR sensor was not found, so similar to the spaceborne systems a regression was done to create a simple payload mass model. The amount of information for airborne systems was much less than the spaceborne systems due to the airborne systems being designed and sold by commercial aerospace companies. The aerospace companies may see the technical specifications of their systems as competitive information, so the technical information is from a limited number of systems. Additionally, since the aperture of these systems was not publicly available, the focal length of the system was used instead.

Name	Focal Length (m)	Weight (kg)
iSky-30HD	0.25	21.5
iSky-50HD	0.72	29
G2030	0.035	0.63
MX-10	0.3	17.2
MX-15	1.5	45

Table 6.5: Airborne Sensor EFL and Weight

From the regression, a model can be determined to calculate the payload mass in kg of an airborne system given its focal length in meters. This equation has an R^2 value of 0.878.

$$payload = 26.2 * focallength + 7.96 \tag{6.19}$$

6.4.3 Ground Station

In order to determine the ground station requirements, the data output from the sensor must be calculated. Image size can be calculated by multiplying the number of pixels by the bit depth to get the number of bits. Then a conversion can be done to get the value in megabytes.

$$imagesize = (crosstrackpixels^2) * \frac{bitdepth}{8 * 1024 * 1024} \tag{6.20}$$

With the image size known, the amount of data per second being generated when imaging can be calculated by multiplying the image size per frame by the frames per second. This will provide data rate per second (in Mb/s).

$$datarate = framerate * imagesize \tag{6.21}$$

The data throughput can then be calculated with the downlink power and all the losses. Dividing the datarate by the throughput gives the single image download

time. With the scan angle and the orbital period, the maximum time that a single ground station can link the sensor is calculated.

$$maxdltime = orbitalperiod * \frac{scanangle}{360} \tag{6.22}$$

To download the full image collected over an area the sensor must be able to link to a ground station for the duration of the single image download time. So conversely, the minimum number of ground stations needed to download the image can be calculated by dividing the single frame download time by the maximum download time and rounding up to the nearest integer. This is assuming that the system downloads the data in real-time via a line of sight link, as opposed to using intersatellite links or downlinking to an aircraft which has line of sight to the ground station.

$$mingndstations = \lceil singledltime/maxdltime \rceil \tag{6.23}$$

6.4.4 Cost

The total cost of each candidate system is broken into two categories, recurring and non-recurring cost. Non-recurring cost include :

- Cost of the sensor
- Cost of the platform
- Cost of ground stations
- Cost to launch into orbit (for satellites)

Since manufacturers don't publish the cost of their systems, in addition to all of their technical specification, adjustments to the sensor cost had to be made. Larger format arrays with large pixels would require large diameter optics in the sensor, which will be more expensive than a comparable system with smaller arrays with smaller pixels. In order to account for this differences in cost, the input values for pixel pitch and cross track pixels are normalized and incorporated into the cost model.

They are both normalized such that the smallest option is equal to one and larger options are greater. The value corresponding to the candidate designs pixel pitch is multiplied with the sensor cost. It is assumed that larger format arrays would contribute to the cost more than pixel size since more pixels would result in a more expensive focal plane and it would result in more expensive optics. So, this value is squared before it is multiplied to the sensor cost. The recurring costs include:

- airborne system operating cost
- annual software maintenance
- operation personnel cost

The airborne system operating cost is the availability multiplied by the containment time of the fire in hours multiplied by the cost per hour of operating the airborne system [61].

$$Cost_{AirborneOperating} = CostperHour_{Operational} * Availability * Time_{FireContainment} \tag{6.24}$$

The annual software maintenance is based off the estimated software lines of code (SLOC) and the cost of full time engineers to support the maintenance efforts. The equation is normalized by 16,000, which is the assumed to be number of SLOC which a typical person can review, as part of a maintenance effort, in a year [61].

$$Cost_{SWMainenance} = \frac{SLOC}{16,000} * N_{FTE} * Cost_{FTE} \tag{6.25}$$

Operation personnel full time cost of the engineers and technicians who support the ground stations for the system. It is assumed that additional ground stations would require additional technicians [61].

$$Cost_{Personnel} = N_{FTE} * Cost_{FTE} + N_{GroundStations} * N_{Tech} * Cost_{Tech} \tag{6.26}$$

6.4.5 Utility Function

There are four design factors, one for each mode or function of remote sensing for wildfire management, which when summed together provide the utility of the entire system. The design factors use sigmoid functions to determine how much utility each of the design factor criteria contribute. The value of using a sigmoid (or S) function is that it caps the utility which a design can get from a single design factor criteria of the design factor with upper and lower bounds. The equation for the sigmoid function used is as follows.

$$y = \frac{1}{1 + e^{-c_1 * (x - c_2)}} \tag{6.27}$$

Prior to using the sigmoid function the input values are adjusted using a base 10 log function to decrease the variation in the data. In this model c_2 is the midpoint of the sigmoid function, which normally is the average of all of the input values. Then c_1 can be calculated using the following equation where k determines whether the function is rising or falling (smaller-is-better, or larger-is-better), g is the growth factor, and $\bar{x}$ is the mean of the input values.

$$c_1 = \frac{k}{g * \bar{x}} \tag{6.28}$$

The growth factor, whether the function is rising or falling, and the midpoint are all dependent on the specific design factor criteria. The growth rate is used to affect the slope of the function, where a higher growth factor results in a higher slope. Rising or falling would depend on whether a larger or smaller design factor criteria would be higher utility. The midpoint is usually the mean of the design factor criteria of the candidate solutions, but could be a different value to prevent the output from skewing. By using the midpoint a differentiation and relative utility score between different architectures is calculated.

Finally, the output values of the sigmoid function are all normalized such that the maximum value is equal to one. This allows each design factor to potentially reach

the value of one. This depends on the difference from the reference value as well as the maximum value set by the inputs to the sigmoid function. The inputs to the sigmoid function are defined in tables 6.6 and 6.7. Graphs of the sigmoid function can be found in the Appendix A.2.

Many of the design factor criteria take in values from real wildfires that occurred to determine the difference between the designed system and what occurred in the real world. For example, the resolution difference is the difference between the candidate designs GSD and the GSD used in the reference fire, or desired by the stakeholders (as determined in the interviews and panel sessions). The imaging rate is a candidate design's swath width multiplied by the velocity, the imaged area is the imaging rate multiplied by the time needed. The download time difference is the difference between the candidate designs download time and a reference download time. The reference values and values from actual fires during each phase are the main contributors to the differences between the utilities from each of the design factors.

$$imagingrate = swathwidth * velocity \tag{6.29}$$

$$imagedarea = swathwidth * velocity * time \tag{6.30}$$

Prediction				Detection			
	k	g	x		k	g	x
imaging rate	1	2	0	imaging rate	1	3	0
time to acquisition	-1	0.9	0	time to acquisition	-1	2	0
availability	-1	0.05	0	availability	-1	0	0.5
resolution difference	1	0.8	0	resolution difference	1	0.5	-1.5
download time difference	1	2	0	download time difference	1	2	0

Table 6.6: Fire Prediction and Detection Utility Parameters

Monitoring				Assessment			
	k	g	x		k	g	x
imaged area	1	10	0	imaging rate	1	2	0
time to acquisition	-1	5	0	time to acquisition	-1	0.9	0
availability	-1	1	0	availability	-1	0.5	0
resolution difference	-1	1.5	0	resolution difference	-1	1.2	0
download time difference	1	2	0	download time difference	1	2	0

Table 6.7: Monitoring and Post-Fire Assessment Utility Parameters

The results from the sigmoid function for each of the design factor criteria is summed, and the result is normalized. To obtain the total utility of a system, all four individual design factor utilities are added together since we assume that each of the utilities for prediction, detection, monitoring, and post-fire assessment are equally useful.

6.4.6 Multiple Systems

In order to account for swarms of UAVs and constellations of satellites, the model includes multiples of systems as shown in figure (left) 6-1. In order to reduce the computing requirements of the model only the top utility designs of each type of platform and sensor are chosen to look at multiples. The model then calculates the utility by comparing the case where the design would be on the same orbit/flight path or on different orbits/flight paths. For same orbit LEO spaceborne candidate designs, it is assumed that the increased systems would be placed an equal angle (true anomaly) apart and therefore be phased evenly on the same orbit. For example for three LEO satellites on the same orbit, they would be spaced 120 degrees apart. This would result in fewer orbits until one of the sensors is over the target area. Specifically, the new revisit time is the old revisit time divided by the number of sensors. No additional ground stations are assumed to be needed since no more than one sensor will be over the target area at a time. For same path airborne candidate designs,

additional systems can be used to fill in for other systems during downtime. Once the rotation of airborne systems has no downtime, additional systems increase the swath width of the candidate design. For different orbit/flight path all candidate designs with increased number of systems would have a wider swath width. Any systems which increase the swath width are assumed to need additional ground stations to support the constant downlink. Any additional systems increase the nonrecurring costs associated with the candidate design.

6.4.7 Mixed Systems

For systems comprised of multiple different sensors, as shown in figure (center) 6-1, the model selects the top candidate designs from airborne, LEO, and GEO for each of the design factor criteria as well as the total utility. This includes multiples of a given system, so the resulting mixed SoS could include multiples of a single candidate design as shown in figure (right) 6-1. The model then goes through a full factorial evaluation of the different chosen systems. For each combination and each function, the spaceborne option is compared to the airborne option. The option with higher utility of the specific design factor is chosen for that function. The result is a system which is comprised of multiple different designs for each design factor. This model doesn't currently consider non-linear effects of mixed systems' cost. The total cost is summed for each of the unique system (or multiple systems), to create the total cost of the mixed system of systems. The utility for each design factor from each system is summed for total mixed system utility.

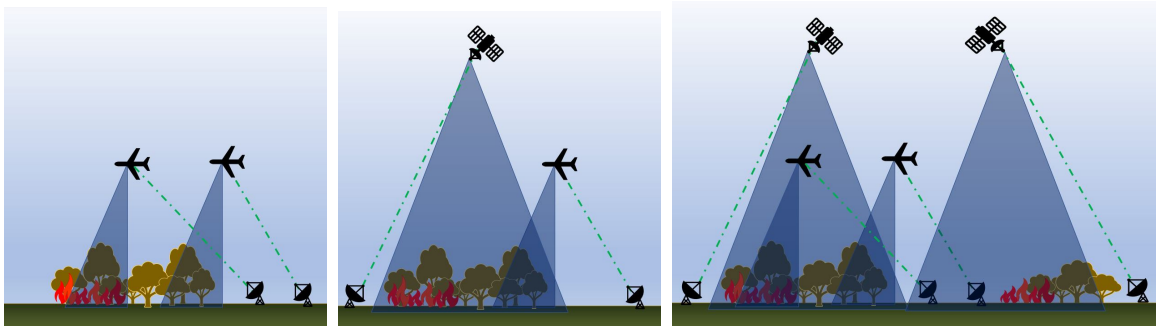

Figure 6-1: Multiple (left), Mixed(center), Multiple and Mixed (right)

Chapter 7

Analysis

Running the model with defined input parameters and variables results in three graphs. The ideal candidate would be on the top left of the graph with maximum utility and minimum cost, see figure 4-1. One graph for each of the design factors utility, and one graph for the total utility of the candidate system of systems design. The x-axis on the graphs is in log base 10 U.S. dollars to more clearly visualize the variation seen among the cost of candidate designs which normally results in many of the candidate designs at a lower price being squished together. A side effect of using a logarithmic function is that smaller cost differences appear even smaller. The index values of the candidate systems are the same in all the different graphs. Multiples of the same system also have the same index, although their total sensors value would be higher. Mixed systems have a unique index, but the systems that they are comprised of can be extracted from the model. The only value that should change for the same index for different graphs is the candidate system's utility.

7.1 Prediction Utility

In the fire prediction utility vs cost graph, there are multiple distinct regions. Remember that fire prediction is about imaging the ground for soil moisture and presence of potential fuel of a future fire (at relatively coarse resolution and not necessarily in real time). On the bottom there is a clustering of spaceborne candidates which all appear

to be LEO satellite designs. The highest utility single system candidate in LEO is a satellite at 2000 km with 4k pixels and 100 meter resolution (this is architecture 533). Directly below that is another LEO system (473) with all the same parameters except it has a 2k pixel array. Increasing the number of the 4k pixel sensors does look to increase the utility of the candidate, but not by enough to bridge the gap to the other clusters of candidates. The candidates with the multiple sensors that fly along the same orbit (526, 10_{so}) appear to have a slightly lower utility than multiple sensors which fly on different orbits(526, 10_{do}) . This is likely because the availability is not as important for the prediction design variable as imaging rate is.

Index	Total Sensors	Utility	Alt (km)	GSD(m)	Pixels	Total Cost (USD)
526	1	0.1948	200	10	4k	3.3M
526	10_{so}	0.2068	200	10	4k	33M
526	$10do$	0.2690	200	10	4k	33M
473	1	0.2264	2000	100	2k	2.9M
533	1	0.2483	2000	100	4k	3.3M

Table 7.1: LEO Candidates' Prediction Utility

The airborne candidates appear to be in one big cluster nearly spanning the width of the graph. On the left of the cluster is one of the cheaper options (31) with an altitude of 10kft and 0.5 m resolution. The highest utility single airborne candidate (519) flies at 30kft with 1m resolution and a 4k pixel array. Multiple airborne sensors do improve the utility in a linear fashion, at a relatively low slope. A candidate with multiple airborne systems, like 519-$10sp$, would function as shown in figure (left) 6-1.

Index	Total Sensors	Utility	Alt (km)	GSD(m)	Pixels	Total Cost (USD)
31	1	0.4552	3.048	0.5	256	1.4M
519	1	0.5808	9.144	1	4k	3.6M
519	10*sp*	0.6343	9.144	1	4k	36M
519	10*dp*	0.6573	9.144	1	4k	37M

Table 7.2: Airborne Candidates' Prediction Utility

The cluster with the highest utility is the one with geostationary orbit sensors (architecture 534). While these have significantly higher utility, they also cost significantly more. Having multiple geostationary sensors does improve the utility but cost increases to a level that is still Pareto optimal but may no longer be attractive to stakeholders who tend to be national or regional (e.g. CalFire) and for them a single geostationary satellite or imager pointed at their territory may be enough. The utility improvement for multiple sensors only applies to sensors with different orbits, since no benefit is seen from having multiple geostationary sensors looking at the same target.

Index	Total Sensors	Utility	Alt (km)	GSD(m)	Pixels	Total Cost (USD)
534	1	.9292	35786	100	4K	54 M
534	10*dp*	1	35786	100	4k	540M

Table 7.3: GEO Candidates' Prediction Utility

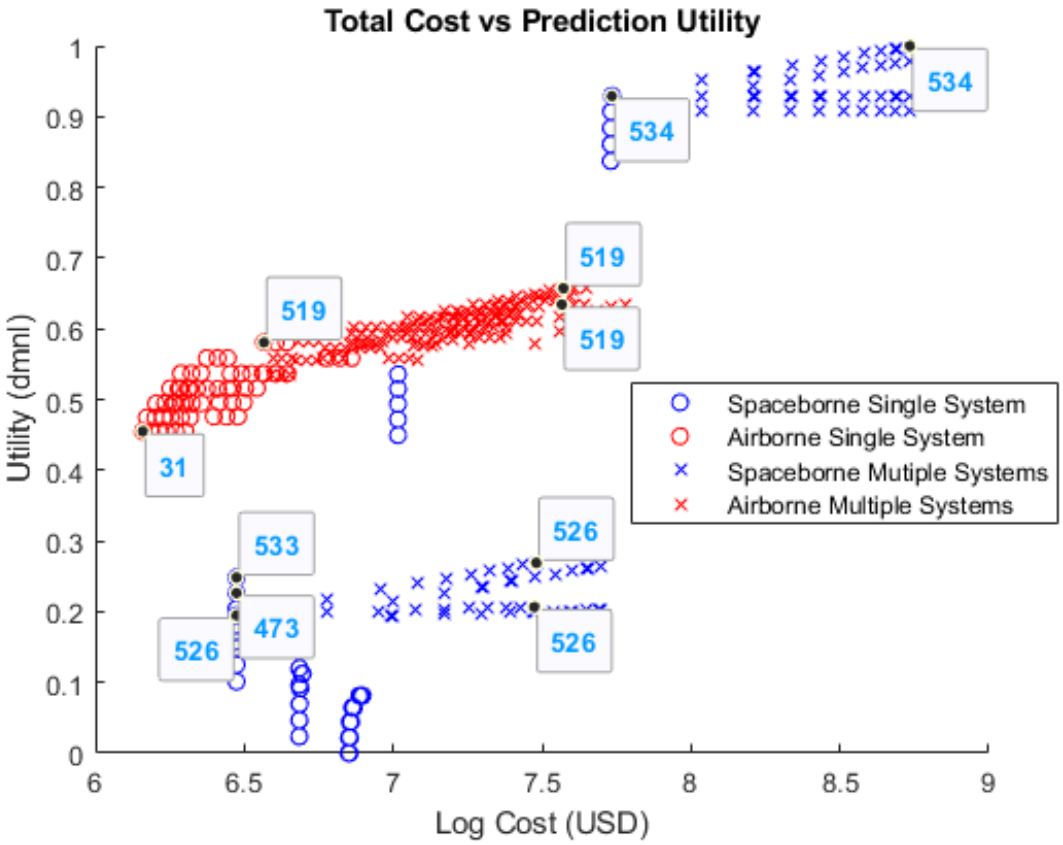

Figure 7-1: Fire Prediction Utility

7.2 Detection Utility

The utility tradespace for fire detection similarly has multiple clusters, see figure 7-2 . Similarly, the low Earth orbit satellites, like index 526, are clustered together with lower utility than all the other candidate designs. This is again likely due to the their higher time to acquisition. Time is critical in fire detection as was seen in the Camp fire where the front was able to move about 6 miles in one hour. If a LEO satellite is on the other side of the Earth when a fire starts, it cannot detect it. The airborne cluster of UAVs again spans the width of the graph and interestingly intersects with the geostationary cluster. Candidate designs in the geostationary cluster, like 534, still have the highest utility but the gap between the geostationary cluster and the multiples of airborne systems is not as large as it was in the prediction design variable's

utility. This is likely because, the smallest GSD for a geostationary system is 100m as opposed to 0.5 meters for the airborne systems. The geostationary orbit systems with smaller GSDs were likely removed from the candidate designs for having too large of a diameter mirror ($>$ 2 m aperture size, about the size of the HST mirror). In order to detect smaller fires and catch them while they're still small, airborne systems would be preferred, but the airborne systems can't be flying constantly. So, unless a lightning storm occurred recently with a potential for sparking one or multiple fires, a geostationary candidate which is available 100% of the time and always on station may be preferred. Most of the candidate designs from the fire prediction which were non-dominated, are also in favorable areas for the fire detection function. However, their relative utility is somewhat different (position of clusters) due to the aforementioned time-criticality of fire detection

Index	Total Sensors	Utility	Alt (km)	GSD(m)	Pixels	Total Cost (USD)
526	1	0.3183	200	10	4k	3.3M
31	1	0.7189	3.048	0.5	256	1.4M
519	1	0.5808	9.144	1	4k	3.6M
519	$10dp$	0.9034	9.144	1	4k	37M
534	1	0.9389	35786	100	4k	54M

Table 7.4: Candidates' Detection Utility

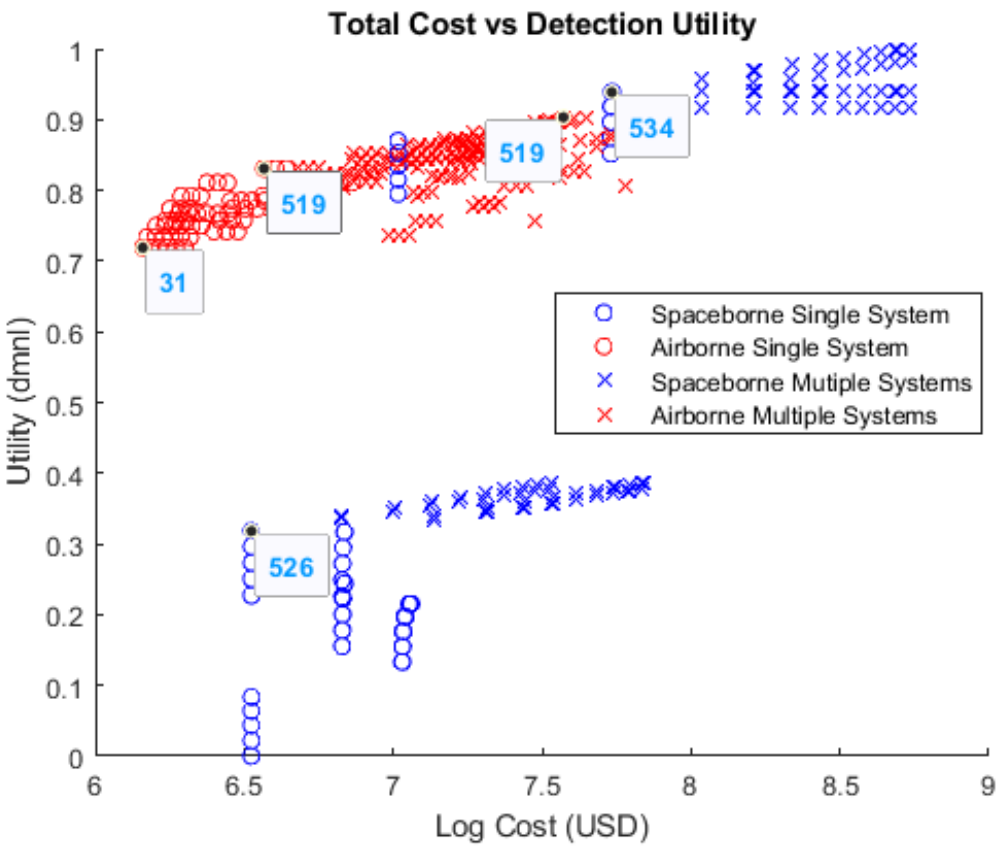

Figure 7-2: Fire Detection Utility

7.3 Monitoring Utility

The fire monitoring design variable utility vs cost graph looks very different compared to the other design variable's graphs. There are distinct clusters similar to the other graphs, but the shapes of the clusters and their respective locations in the monitoring tradespace differ from the other cases of prediction and detection. The low Earth orbit candidates, like 526, again are low utility likely due to their low availability and high time required to acquire imagery. Interestingly, the geostationary orbiting candidate designs, like 534, are also lower utility and not on the Pareto frontier. This is likely due to their significantly larger GSD when compared to the airborne systems. The airborne candidate designs, like 519, encompass the entire Pareto frontier likely due to their comparatively small GSD and high availability. Additional airborne systems

increase the candidate design's total availability, and when they are put on a different path increase the imaging rate. These traits are highly desirable when monitoring an active fire. This finding matches our intuition which is that during an active fire, airborne platforms circling at about 9-10 km above the active fire would provide the best resolution and most timely imagery, assuming the imagery can be relayed to the ground in near real time.

Index	Total Sensors	Utility	Alt (km)	GSD(m)	Pixels	Total Cost (USD)
526	1	0.3040	200	10	4k	3.3M
31	1	0.7465	3.048	0.5	256	1.4M
519	1	0.9287	9.144	1	4k	3.6M
519	$10dp$	1	9.144	1	4k	37M
534	1	0.8872	35786	100	4k	54M

Table 7.5: Candidates' Monitoring Utility

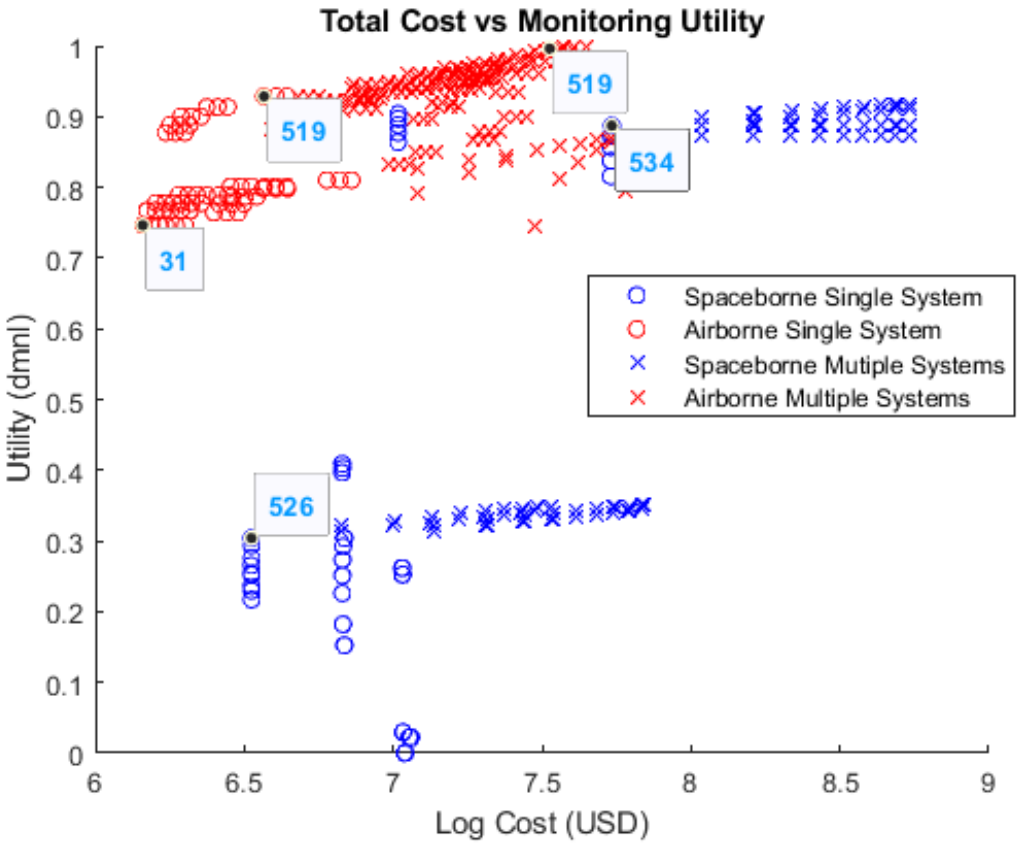

Figure 7-3: Fire Monitoring Utility

7.4 Assessment Utility

The post-fire assessment tradespace graph is similar to the fire prediction one, which makes sense since there are many functional similarities between the two. The low Earth orbit candidate designs, like 526, have a slightly lower utility for the assessment design variable than they did for the prediction design variable. Since there is more of an urgency to get data after the fire compared to assessing the ground before a potential fire, the lower relative utility scores for LEO candidates, which have a higher time to acquire, are expected. The airborne candidate cluster, including 519, and geostationary orbit candidate cluster, including 534, also have similar relative locations to their locations in the prediction design variable graph. At lower costs, airborne candidates have a higher utility, but at higher costs the spaceborne geosta-

tionary satellite candidates have higher utility. This is mainly because geostationary satellites are always available day or night and are always on station. Note that a Log Cost (USD) of 8 corresponds to $100 million.

Index	Total Sensors	Utility	Alt (km)	GSD(m)	Pixels	Total Cost (USD)
526	1	0.1378	200	10	4k	3.3M
31	1	0.6029	3.048	0.5	256	1.4M
519	1	0.6916	9.144	1	4k	3.6M
519	$10dp$	0.7458	9.144	1	4k	37M
534	1	0.9499	35786	100	4k	54M

Table 7.6: Candidates' Assessment Utility

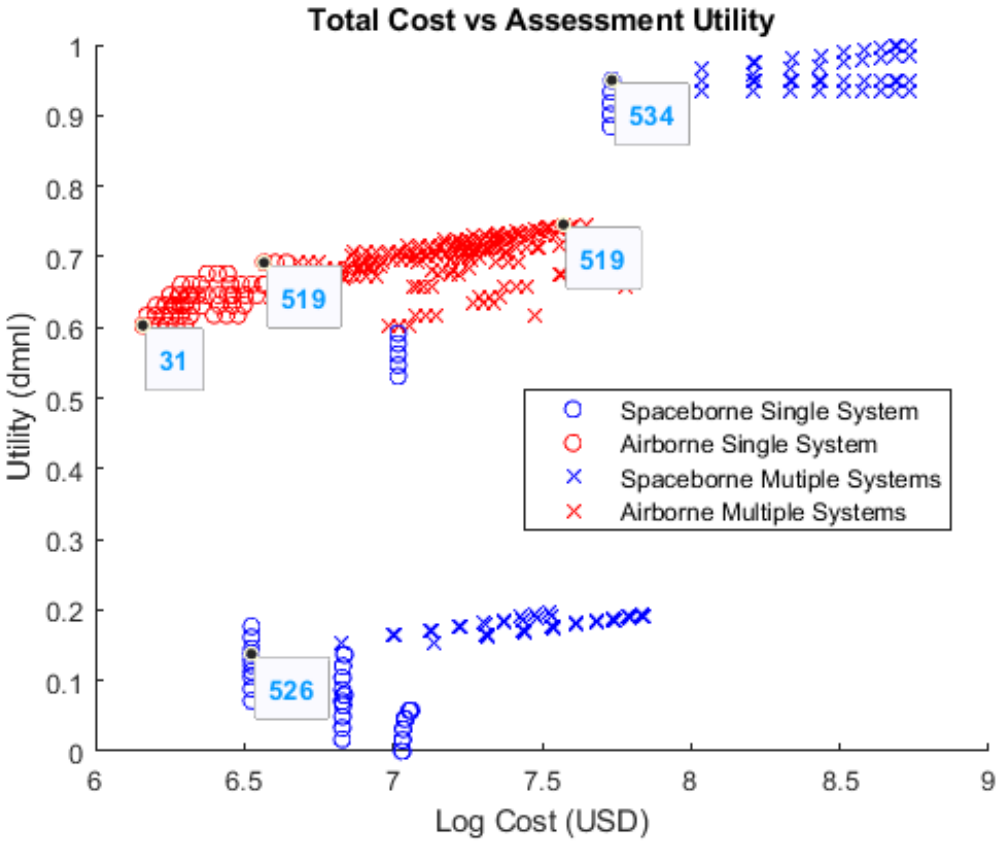

Figure 7-4: Post-Fire Assessment Utility

7.5 Overall Utility

The overall utility of the design candidates has similar clustering to some of the other individual tradespaces for prediction, detection, monitoring and post-assessment. Additionally, mixed systems are included in this graph. Low Earth orbit candidate designs, like 526, which have been consistently lower utility, have an overall lower utility. It seems that LEO satellites for fire monitoring are only attractive when they form a continuous coverage constellation or sensors could piggyback on existing constellations (e.g. Starlink). The airborne candidate designs, like 519, all have higher utility than the LEO candidates with some at a lower cost. At higher costs, there is a cluster of geostationary orbit satellites, like 534, which have a higher overall utility.

Index	Total Sensors	Utility	Alt (km)	GSD(m)	Pixels	Total Cost (USD)
526	1	0.9549	200	10	4k	3.3M
31	1	2.5325	3.048	0.5	256	1.4M
519	1	3.0320	9.144	1	4k	3.6M
519	$10dp$	3.3066	9.144	1	4k	37M
534	1	3.7052	35786	100	4k	54M

Table 7.7: Candidates' Overall Utility

The mixed systems are constructed from the top ten aircraft, LEO satellites, and GEO satellites for each of the design variables as well as the total utility. Since the top ten also included multiples of a given system, all of the top ten are using larger quantities of systems. This resulted in the the mixed systems all being higher cost, but some having a higher utility than any of the other individual designs. The least expensive mixed systems design that is on the Pareto frontier , SoS candidate 3634, costs an estimated 518M USD. This system of systems would be comprised of 9 geostationary orbit satellites with 100m GSD looking at different locations in the U.S., as well as 8 aircraft with 1m GSD. This system would resemble the mixed

systems with multiples of a system as shown in figure (right) 6-1. The larger number of geostationary satellites is likely due to the fact that there is no sigmoid function associated with the utility the certain swath width, which could limit the size of the sensor swath. The model geostationary orbit satellites would be used for all but the monitoring, and the aircraft would be used exclusively for the monitoring of active fires. Technically with an SoS comprised of both, aircraft could be deployed post lightning storm as a secondary system to search for small fires and the geostationary satellite could be used as a primary system to monitor the full scope of the fire.

Design Variable	Index	Total Sensors	Utility	Alt (km)	GSD(m)	Pixels
Prediction	534	$9dp$	0.9969	35786	100	4k
Detection	534	$9dp$	0.9975	35786	100	4k
Monitoring	519	$8dp$	0.9921	9.144	1	4k
Assessment	534	$9dp$	0.9978	35786	100	4k

Table 7.8: Index 3634 Systems

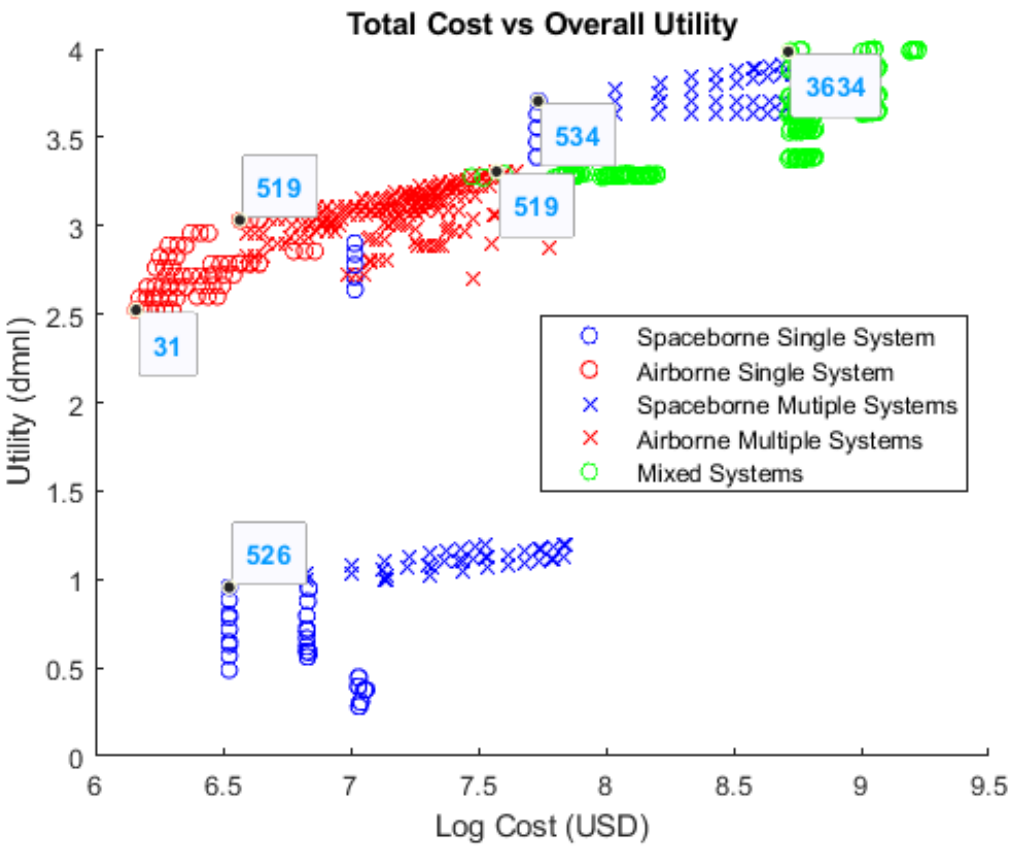

Figure 7-5: Overall Utility

7.5.1 Other Wavelengths

To account for a multi-spectral sensor, with focal planes that can detect different wavelengths of light, the model was run at different wavelengths. The optics and other sensor parameters from the top candidate systems were then incorporated into these runs. Due to the different wavelength, the GSD of the sensor was different from the initial run. For shorter wavelengths, the GSD was smaller and for larger wavelengths, the GSD was larger. From the initial run of the model, the top candidates were near the top on almost all of the design factors. This was also the case for the other wavelengths. So, for additional wavelengths, only the overall utility is looked at.

Red Band

The 0.650 micrometer wavelength is the red band in the visible spectrum. This would be used for fuel detection before a fire is ignited and could support in fire detection as it occurs. From the initial run, one of the SoS candidates which was looked at was index 3634. This was comprised of airborne system 519 and spaceborne GEO system 534. When input into the model for the red wavelength, both individual systems are still on the Pareto frontier. They both also have a smaller GSD which provides them a higher spatial resolution than similar systems. This is because the larger SWIR wavelength used in the initial run required larger optics for the same GSD. Since Red is a shorter wavelength than SWIR, smaller optics can be used to acquire the same GSD. As a result, the systems from the initial run cost more than similar systems for the red wavelength alone. Note that the utilities here are greater than 1.0 since we are adding the individual utilities from multiple wavelengths and not re-normalizing the results to 1.0.

Index	Total Sensors	Utility	Alt (km)	GSD(m)	Pixels	Total Cost (USD)
3	1	2.5621	9.144	0.5	256	2M
519	1	2.8209	9.144	0.4	4k	3.6M
504	1	3.6460	35786	100	4k	24M
534	1	3.7122	35786	38	4k	54M

Table 7.9: Candidates' Red Overall Utility

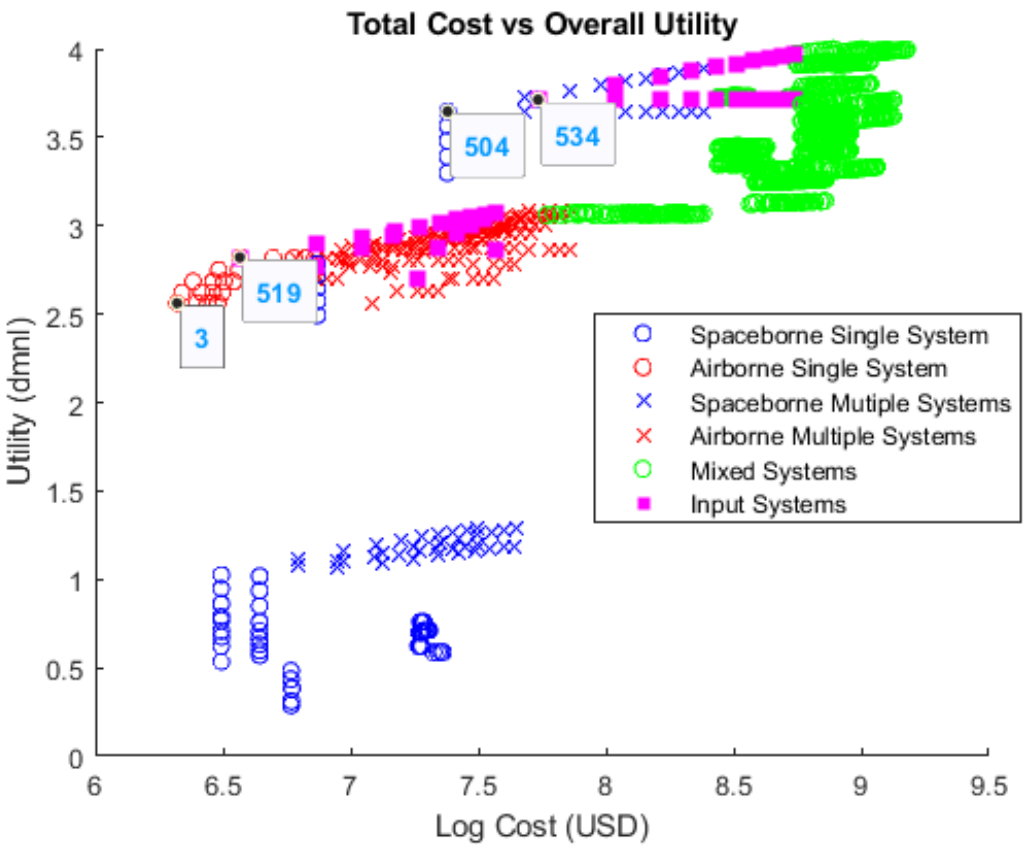

Figure 7-6: Red Band Overall Utility

MWIR Band

The 3.5 micrometer wavelength is in the midwave infrared band. This would be used primarily for detection and monitoring of wildfires. Systems 519 and 534 are still on the Pareto frontier, but have much larger GSDs than comparable systems. Again, this is due to the difference in the size of the optics required for a given GSD. The difference in the optics requirements results in the systems from the initial run less expensive than comparable systems for the MWIR band.

Index	Total Sensors	Utility	Alt (km)	GSD(m)	Pixels	Total Cost (USD)
37	1	2.6758	3.048	1	256	1.1M
519	1	3.0843	9.144	2	4k	36M
534	1	3.6247	35786	206	4k	54M
564	1	3.6925	35786	100	4k	109M

Table 7.10: Candidates' MWIR Overall Utility

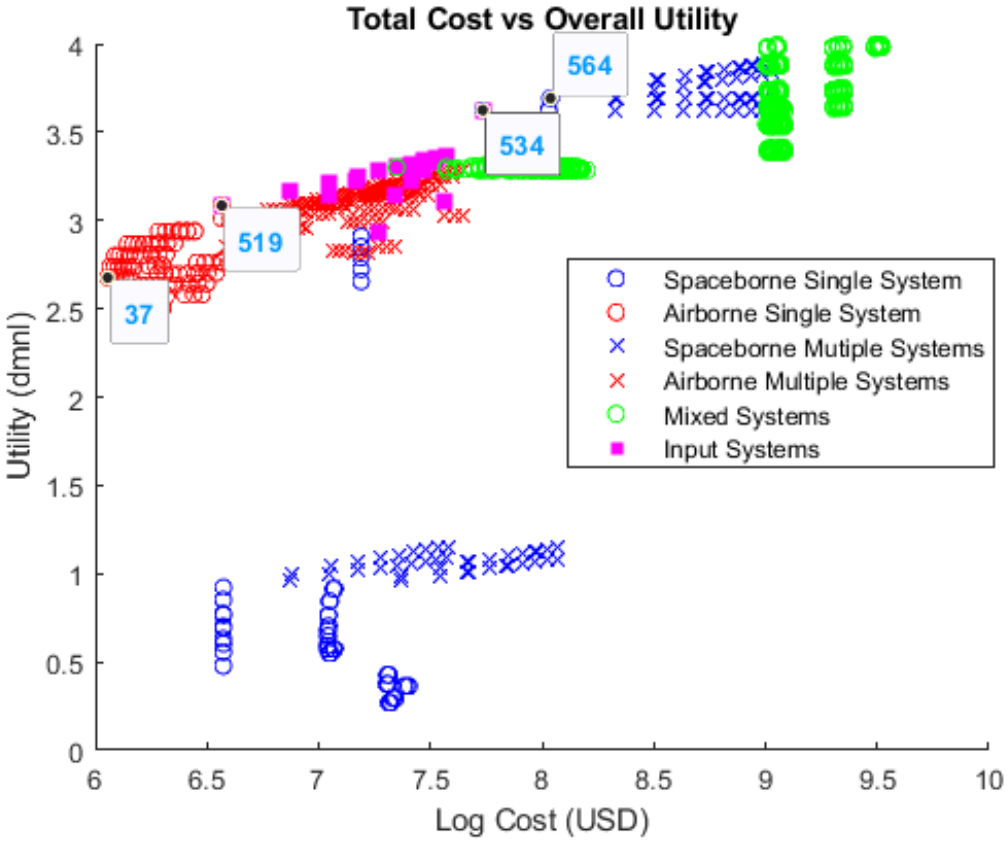

Figure 7-7: MWIR Overall Utility

LWIR Band

The 10.6 micrometer wavelength is in the long wave infrared band. Similar to the midwave band, this wavelength would be used for detection and monitoring. Since the

optics from systems from the initial run provide comparatively larger GSDs for this wavelength, their utility is not high enough for them to be on the Pareto frontier. Unlike the other bands, none of the geosynchronous satellites are on the Pareto frontier in the LWIR band. This is likely because the optics required for small enough GSD for firefighting for GEO satellites are larger than the cutoff threshold in the model of 2m diameter. So, the remaining GEO systems, aside from system 534, have 1000m GSD. So, the mixed SoS candidate, 6867, is comprised of only airborne systems. The higher altitude system with a larger GSD is doing the prediction, detection, and assessment, which was delegated to GEO satellites for other bands. The system which is at a lower altitude and smaller GSD is used for active fire monitoring. Since this SoS is just comprised of aircraft, the total cost is much lower at 28M USD. While this SoS does provide a higher utility than the output of the model run using the SWIR band, without the GEO satellite detection operations to be carried out 24/7 would be more challenging. The aircraft would need to be continually flying over the target area for detection, which would be expensive and challenging to manage.

Index	Total Sensors	Utility	Alt (km)	GSD(m)	Pixels	Total Cost (USD)
577	1	3.3950	3.048	1	4k	3.3M
585	1	3.5803	9.144	10	4k	1.2M
519	1	3.5828	9.144	6.2	4k	3.6M
600	1	3.1955	35786	1000	4k	35M
534	1	3.2017	35786	623	4k	54M

Table 7.11: Candidates' LWIR Overall Utility

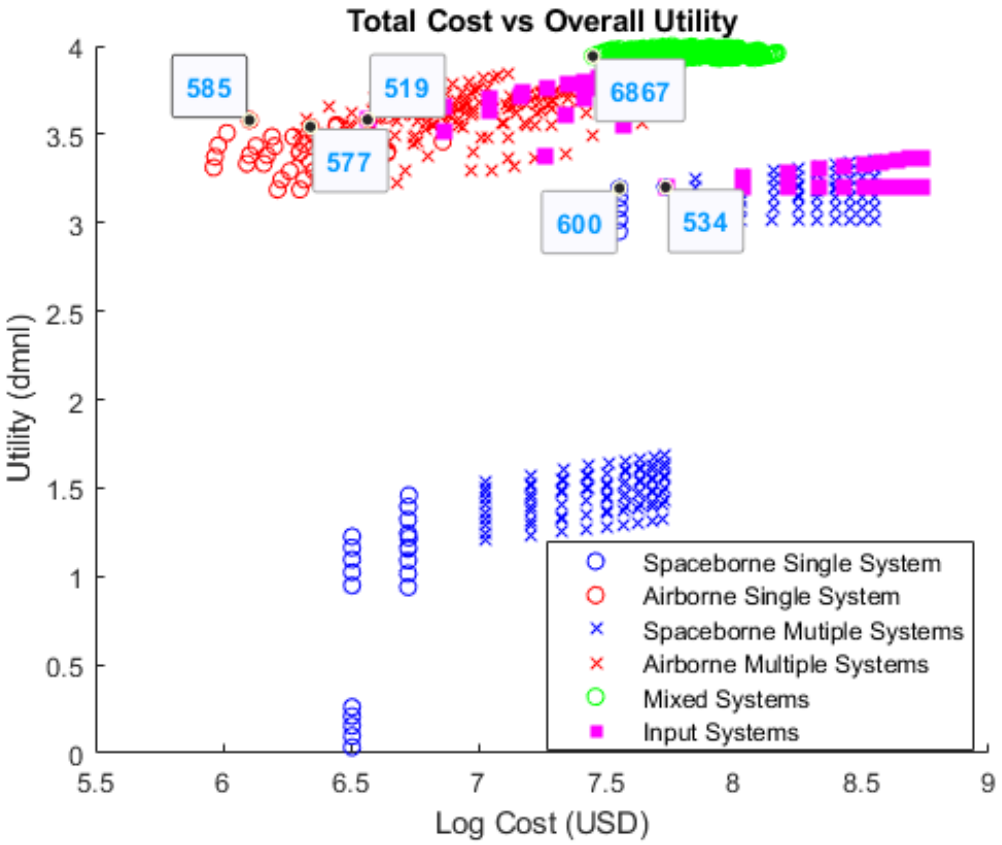

Figure 7-8: LWIR Overall Utility

Design Variable	Index	Total Sensors	Utility	Alt (km)	GSD(m)	Pixels
Prediction	585	6*dp*	0.9864	9.144	10	4k
Detection	585	6*dp*	0.9865	35786	10	4k
Monitoring	577	9*dp*	0.9782	9.144	1	4k
Assessment	585	6*dp*	0.9905	9.144	10	4k

Table 7.12: Index 6867 Systems

7.6 Comparison to Current and Other Systems

The Sentinel 2 and Landsat are both polar orbiting satellites. Their altitude allows them to acquire imagery with up to 20m resolution and 30m resolution, respectively.

But due to their orbit, they can have up to 16 day revisit times (depending on the latitude of the target) which are even longer than the LEO satellites in the model. A similar system in our analysis would be candidate 556, with 0.15 m diameter aperture at 200km altitude, and 25 hour revisit time. This means that the information that they are able to gather won't be useful for immediate decision making in fire management. As a result, the utility from these systems, with close to 90 degree inclination, would likely be lower than the LEO cluster in the model, with close to 45 degrees in inclination in a repeating ground track orbit. Ground based systems like fire towers have other fire management functionalities outside of the scope of this model, but in regard to the design variables they primarily focus on fire detection and fire monitoring. They don't neatly fit into the model, but even though they have a wide field of view their ability to spot fires is limited to the capability of their binoculars. A comparable system might have a large swath width and a large GSD. The watch towers are normally placed one every 100k acres. When paired with multiple remote automated weather station (RAWS), the pair would be capable of performing in each one of the design variables. The RAWS are meant to be placed every 5km [33], so approximately 100 would be needed to cover the area of a fire watch tower. The total cost of that system of systems would be 2.100M USD putting it close to the range of cost of the cheaper candidates in the model. Given the fact the towers are stationary, their time to acquisition would be either zero, or infinite, since they are unable to move to gather more information about a fire out of range. With a high GSD and maximum time to acquire of infinity, this system of systems would have a very low utility. In 2013 UC Berkeley proposed the creation of a geosynchronous satellite called Fire Urgency Estimator on Geosynchronous Orbit (FUEGO) [53]. This satellite would be equipped with a 4k pixel detector on a sensor with 0.5m diameter which would have a 72 m GSD. The specifications of this proposed satellite are very close to the specifications of the GEO satellite in the optimal candidate from our overall utility graph. FUEGO was estimated to cost "hundreds of millions of dollars" compared to the optimal candidate's 55M. The GOES-U geostationary earth observation satellite, which is expected to launch in 2024, cost hundreds of millions just for launch costs

alone, so there are likely additional costs which need to be added into both models [48]. But the information in the model should be enough for ranking the candidate systems. It is possible that there were additional costs that were factored into their modeling.

A similar system would be candidate 555 which has 0.5m diameter optics, is located in a geosynchronous orbit and has a 4k by 4k pixel focal plane. The smaller optics when compared to 534 puts it at a slightly lower utility due to larger GSD. But the fact that a GEO satellite, with similar properties, was close to optimal in their research is significant. Still, a geostationary satellite may not have the resolution to detect at a 1 m^2 target as requested by the stakeholders for active fire events. To fulfill that requirement the airborne systems in the optimal architecture are needed. So FUEGO alone, would not be able to have a higher utility than our optimal SoS (denoted in the figure below as 3834).

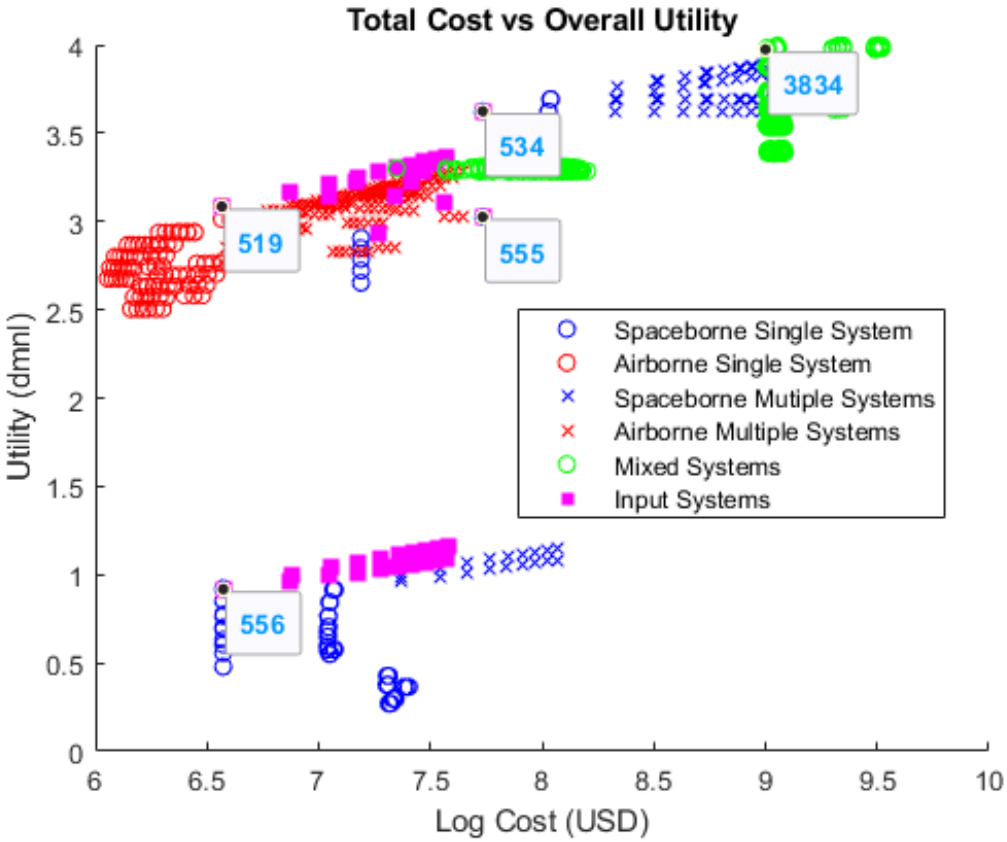

Figure 7-9: Overall Utility Comparison to Other Systems

This chapter conducted a detailed tradespace analysis for airborne and spaceborne wildfire management systems at different wavelength bands and covering the phases of pre-fire prediction, fire detection, fire monitoring, and post-fire damage assessment. The next chapter summarizes the conclusions and recommendations for future work.

Chapter 8

Conclusion

8.1 Findings

In recent years the fire seasons have gotten increasingly expensive and more damaging. This is a worldwide phenomenon driven by climate change and is particularly acute in some areas like California.

Due to climate change, it is expected that this will only get worse. Remote sensing can be used to predict likelihood that a fire will occur in a given area. It can also detect when a fire has occurred, monitor a fire's spread, and assess the situation post fire to help prevent further damage from occurring. The fire management community is looking for remote sensing systems that can provide more accurate data and communicate that data in real time. They are also looking for systems that can gather data before, during, and after the fire.

Current remote sensing systems are *not* able to meet the needs of those supporting the fire detection and management efforts. This is due to the fact that most of the systems used are not designed with fire detection and management as their primary use case. Especially during the monitoring phase real time data at 1 m resolution in the infrared regime is particularly useful. However when fires are not burning a lower resolution and more continuous monitoring are required. By using tradespace analysis, multiple design candidate architectures can be simultaneously compared. The model developed here incorporated both airborne and spaceborne sensors at

different altitudes, different detecting elements, and different optics. By looking at the Pareto frontier, the optimal designs for a given cost could be extracted. The key findings are as follows:

- Candidates with satellites orbiting at low Earth orbit had relatively low utility and higher costs when compared to airborne systems. An example for this is architecture 526 which could provide a good GSD of 10 m, but not provide continuous monitoring.

- Candidates with geostationary satellites had the highest utility except for when monitoring active fires. The candidates with geostationary orbiting satellites were also among the most expensive. A typical geostationary satellite of high value is architecture 534 with a 4k x 4k pixel array and a 100 m GSD. At larger wavelengths, like the thermal band, the optics to get a 100m GSD require optics larger than 2m in diameter. There are very few remote sensing optical telescopes which have diameters larger than 2 meters.

- Candidates with airborne sensors offered a relatively high utility and had a wide range in cost. An interesting distinction is to be made between low flying UAVs at 3 km altitude (e.g. architecture 31) and higher flying UAVs at 9 km altitude (e.g. architecture 519). In general the higher flying UAVs provide more utility since they cover a wider swath, carry more payload and have longer endurance. Additionally, these higher flying UAVs would avoid being hit by slurry (water with additives) discharged from lower flying fire-fighting aircraft. It would be interesting to investigate if some retired U.S. military high altitude drones that were used in overseas missions could be repurposed for domestic firefighting operations.

- It was found that, a mixed system of systems consisting of multiple airborne sensors and multiple geostationary orbiting satellites had the highest utility (architecture 3634). This type of mixed system would cost an estimated 518M USD.

A mixed system, such as ID 3634, would primarily use geostationary orbiting satellites for prediction, detection and assessment of wildland fires and be on station 24/7. The airborne sensors would be primarily used for monitoring active fire events and be launched "on demand". Both systems could also be used as secondary systems in each task. Putting such a system of systems in place would allow wildland fires in the Western U.S. to be detected while they're still small, reducing the effort needed for suppression. Data on the fuels and soil moisture for a given area would be much more recent and available in real time allowing for more informed decision making.

Active fires could also be monitored in real time at high resolution, allowing for a better understanding of the fire behavior. Feeding this information into a fire behavioral model would allow for more accurate prediction of the spread of the active fire. More accurate predictions would help firefighting teams operate in a safer environment, and help the fire management deploy more accurate evacuation notices. This system can be continually scaled up by acquiring additional satellites or aircraft as needed.

8.2 Future Work

The modeling efforts were constrained by the lack of certain information that, if available, could have improved the accuracy of the model. This section summarizes some potential future work:

- Cost models which include more parameters, aside from just aperture diameter, would have been useful to more accurately differentiate the candidates by cost.
- The weight estimations which were used to calculate the launch cost or platform cost were constrained by the data on available systems. Airborne systems in particular were difficult to find information on.
- Focal planes were also difficult to find technical specifications or cost information on. The model only looked at sensors operating in a pushbroom mode. Sensors operating in a whiskbroom mode may be able to perform at a similar level but

with a smaller detecting array. Determining how to model this type of sensor and incorporating it into the tradespace may add some interesting datapoints.

- LIDAR was a technology that was mentioned multiple times that stakeholders were interested in for its capability to determine fuel structure in a forest. This sort of active remote sensing was not incorporated into this model, but could lead to a more advanced system of systems.

- , Finally, a new type of flight platform, high altitude stratospheric solar-powered drones such as the Airbus Zephyr have recently been deployed, and have established a world record of being aloft at altitudes of about 20 km for 26 days without burning any fuel. While those platforms can only carry small payloads on the order of 10 kg today, they could become an effective alternative between high altitude UAVs and low Earth orbit satellites. These systems, sometimes referred to as "High-altitude Pseudo-Satellites" (HAPS), could be incorporated in future tradespace analysis.

While the problem of wildfires is getting worse, our technological toolkit is also growing rapidly. This thesis has conducted a systematic analysis of the tradespace for systems of systems for wildfire prediction, detection, monitoring and post-fire assessment using a system of systems of airborne and spaceborne platforms and clearly points to some promising areas for future investments.

Appendix A

Figures

A.1 Orbital Paths

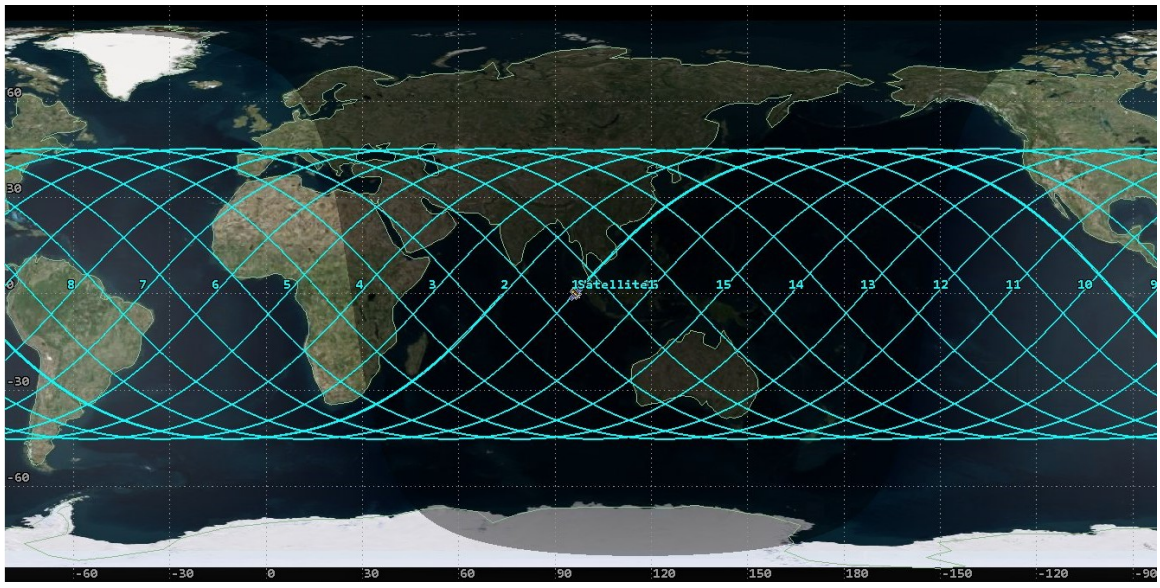

Figure A-1: Orbital path of 200km 45 degree inclination LEO Satellite Candidate

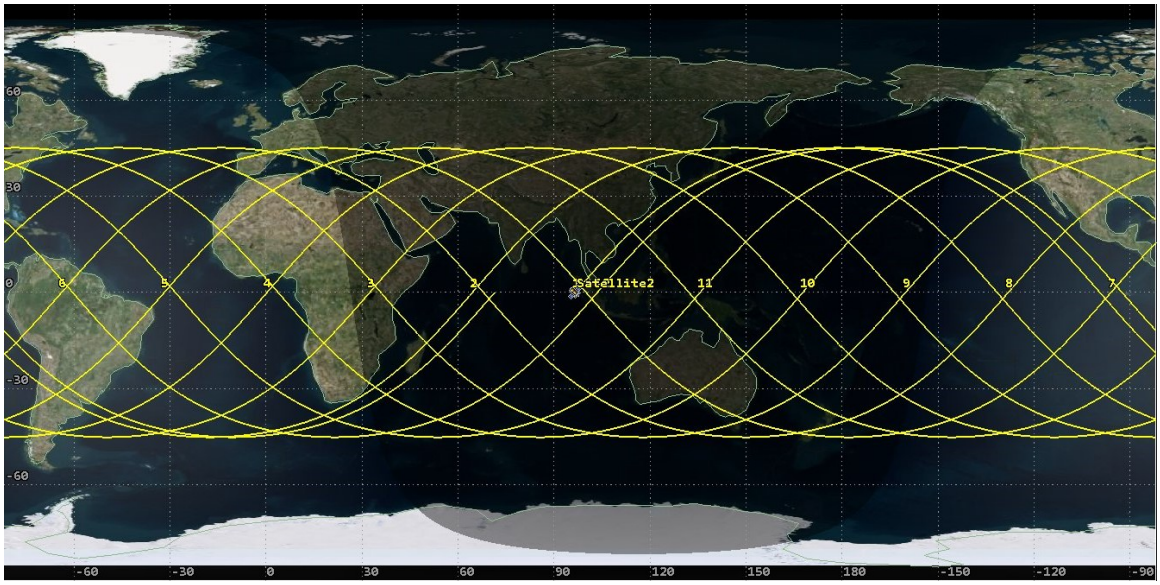

Figure A-2: Orbital path of 2000km 45 degree inclination LEO Satellite Candidate

A.2 Utility Curves

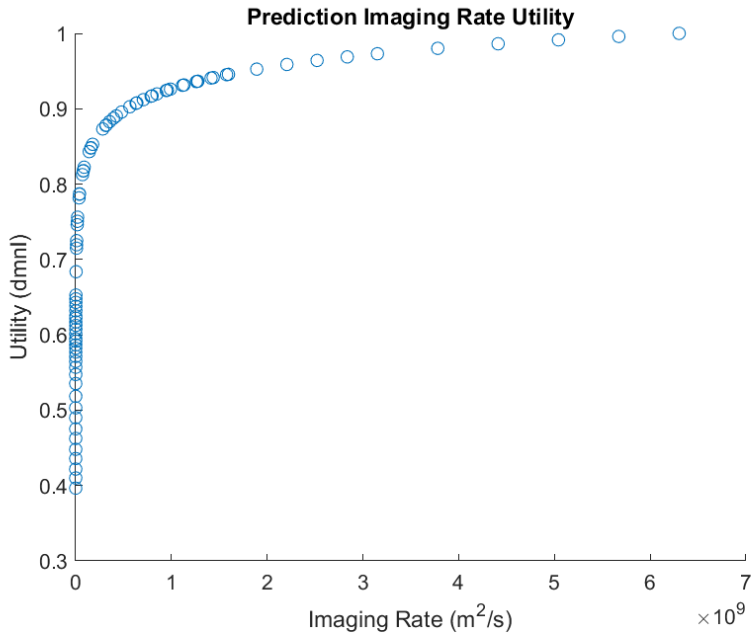

Figure A-3: Prediction Imaging Rate Utility

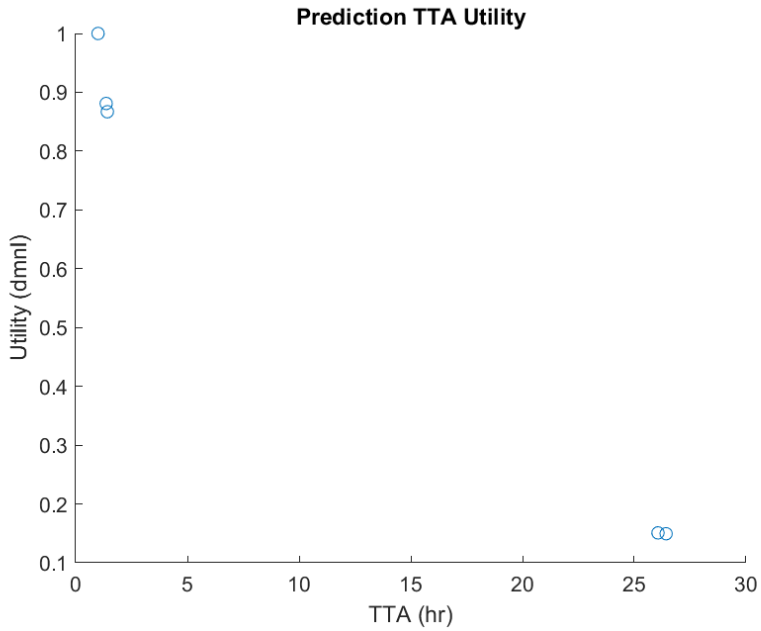

Figure A-4: Prediction TTA Utility

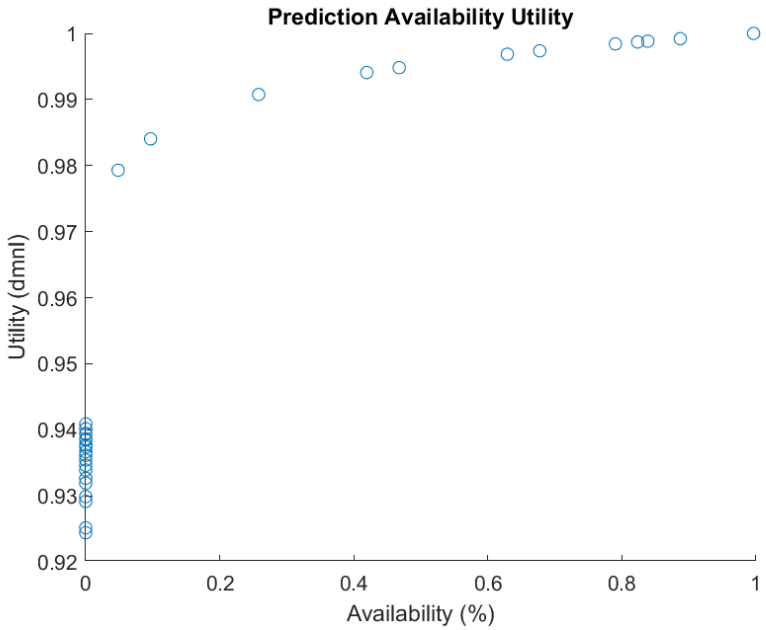

Figure A-5: Prediction Availability Utility

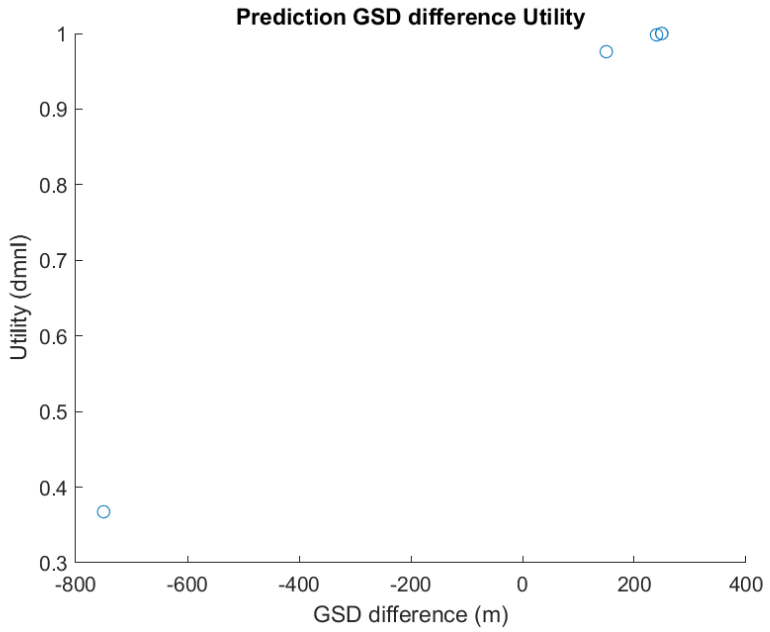

Figure A-6: Prediction GSD Utility

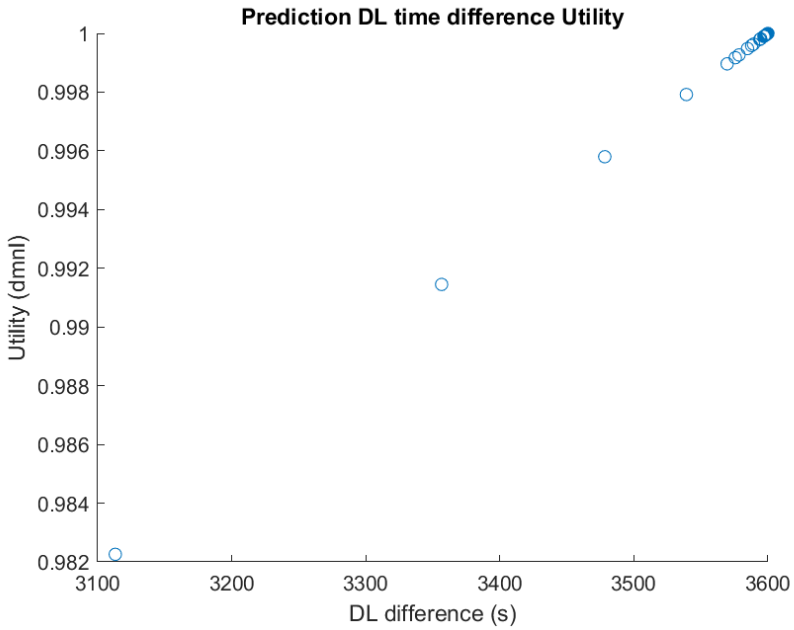

Figure A-7: Prediction DL Utility

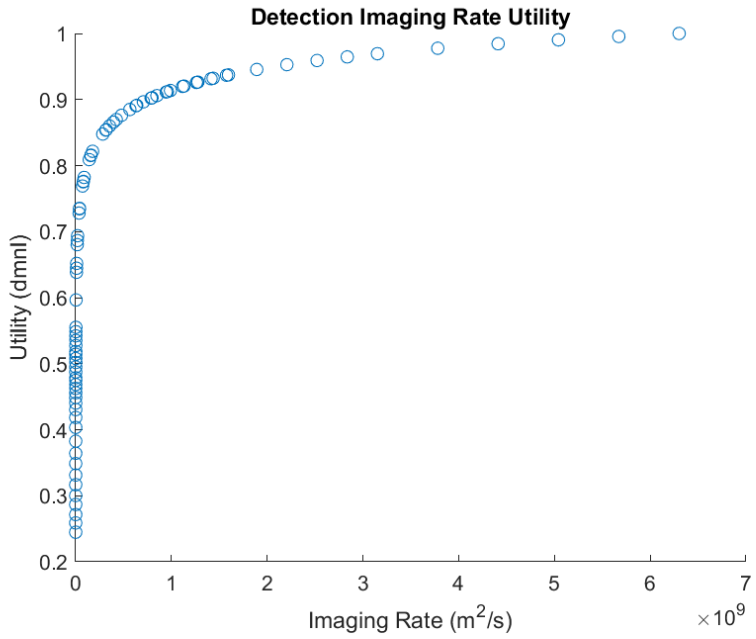

Figure A-8: Detection Imaging Rate Utility

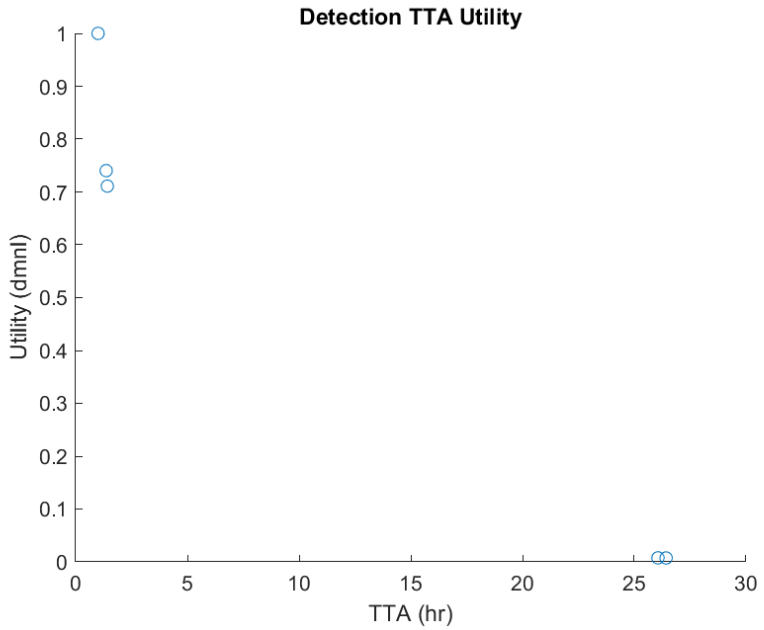

Figure A-9: Detection TTA Utility

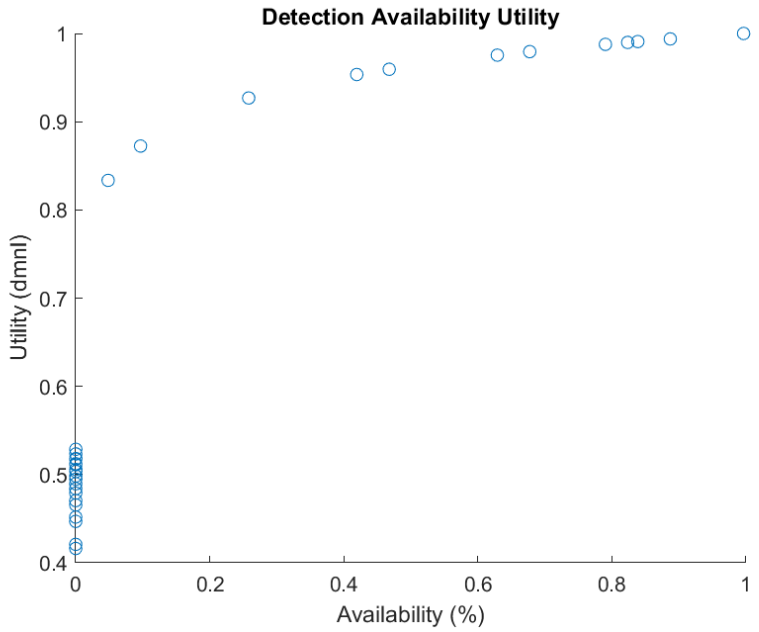

Figure A-10: Detection Availability Utility

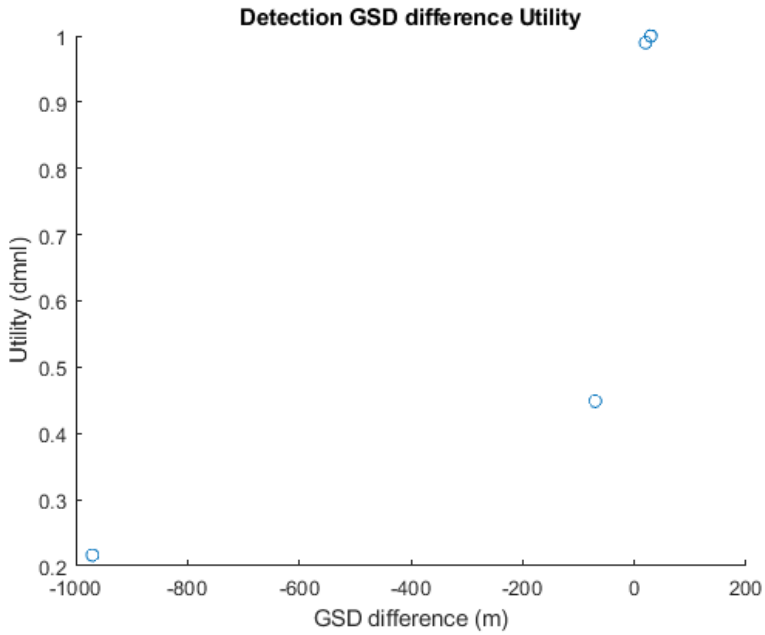

Figure A-11: Detection GSD Utility

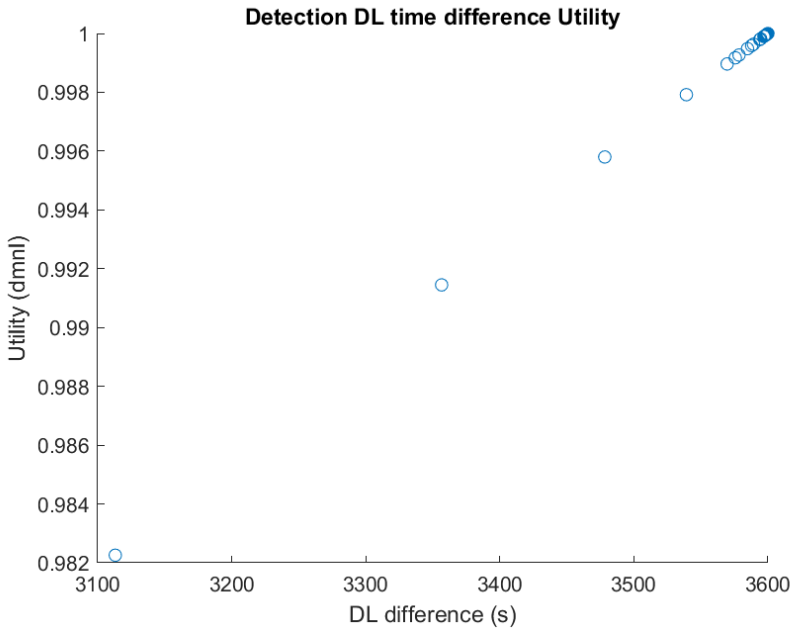

Figure A-12: Detection DL Utility

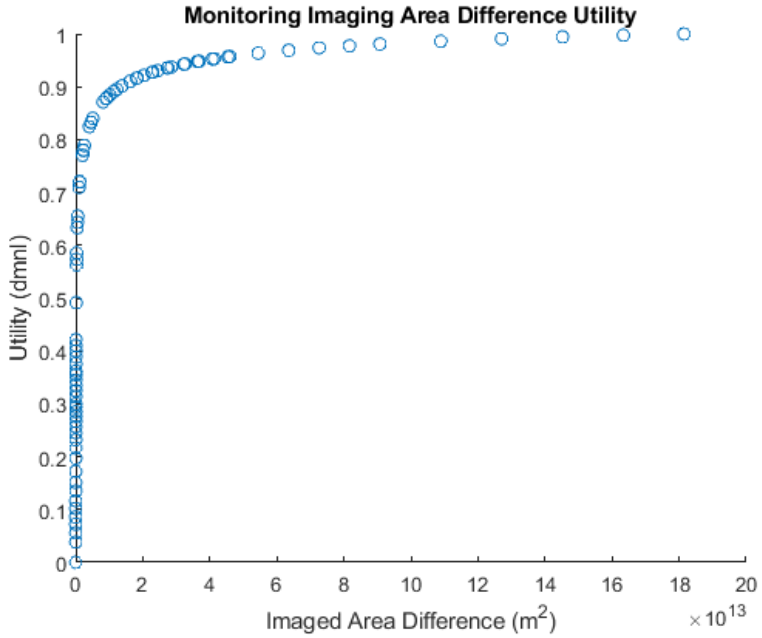

Figure A-13: Monitoring Imaged Area Utility

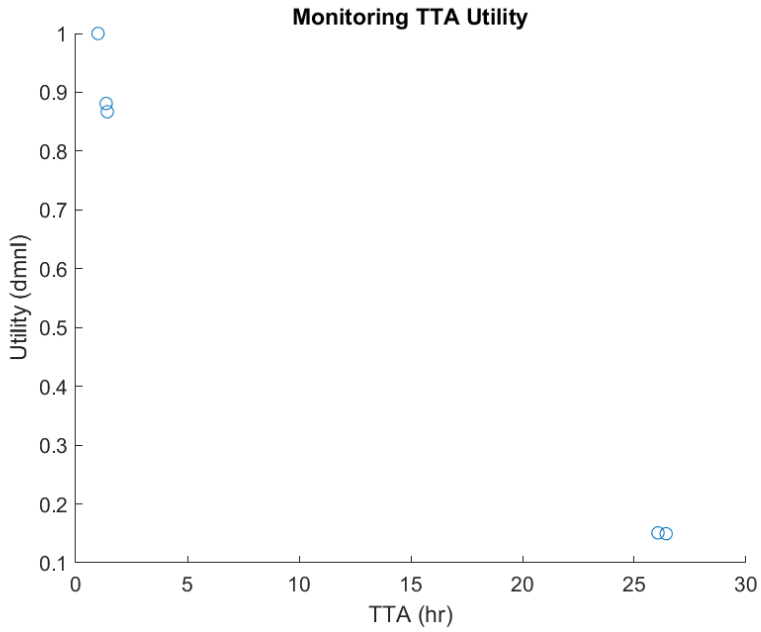

Figure A-14: Monitoring TTA Utility

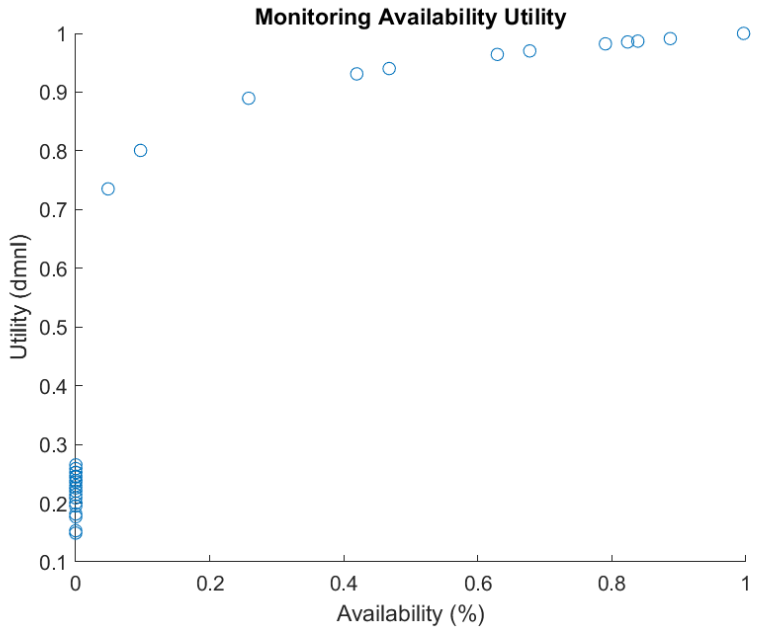

Figure A-15: Monitoring Availability Utility

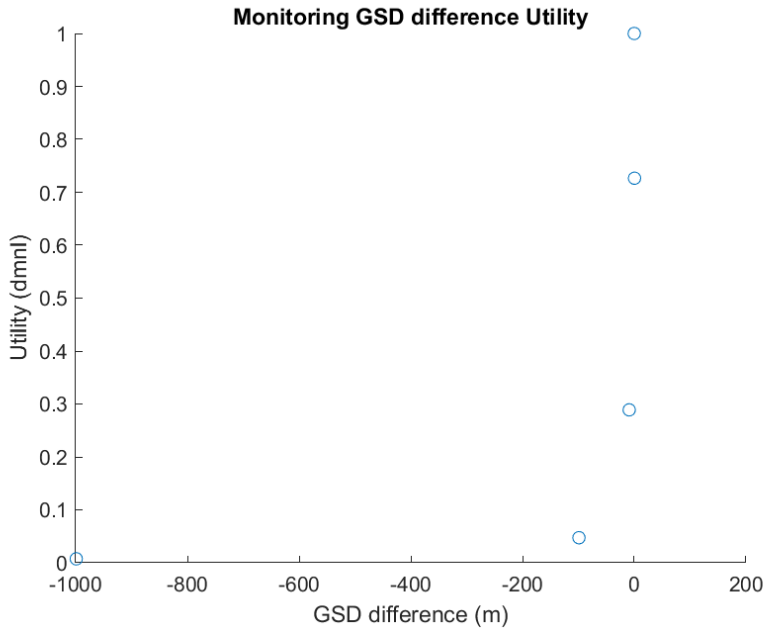

Figure A-16: Monitoring GSD Utility

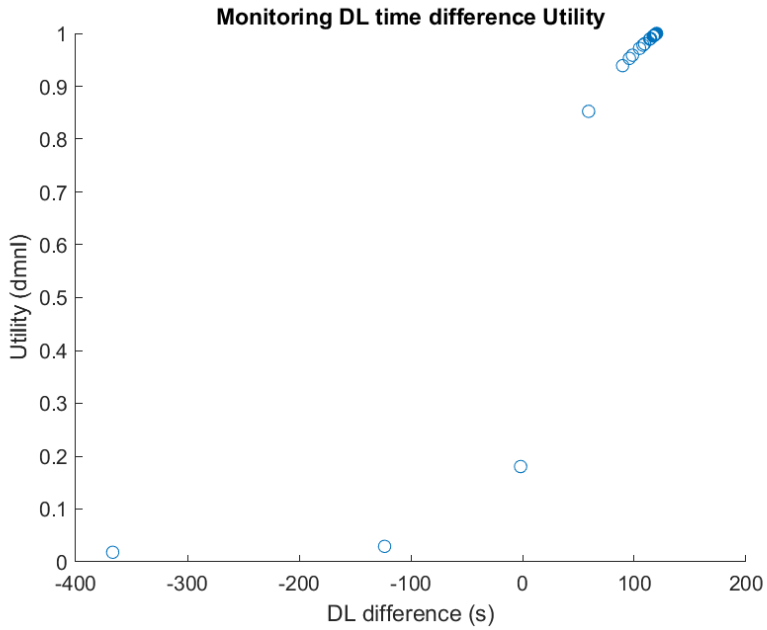

Figure A-17: Monitoring DL Utility

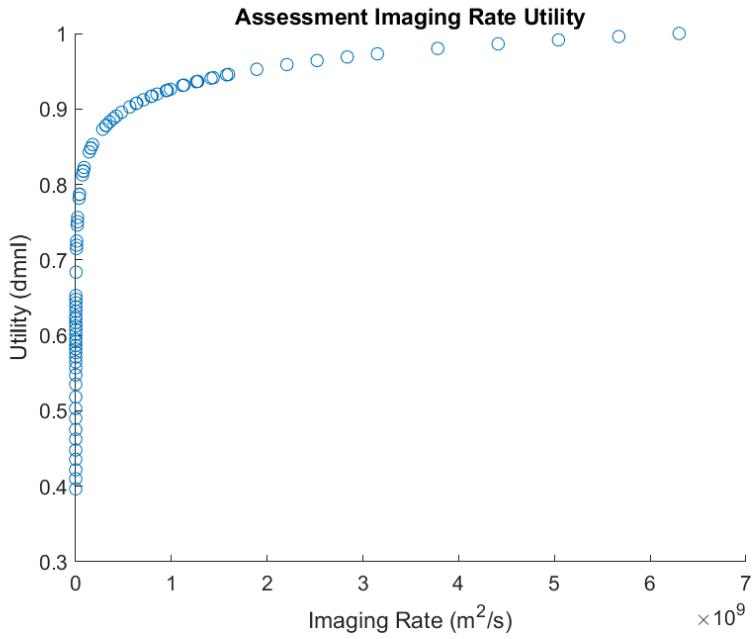

Figure A-18: Assessment Imaging Rate Utility

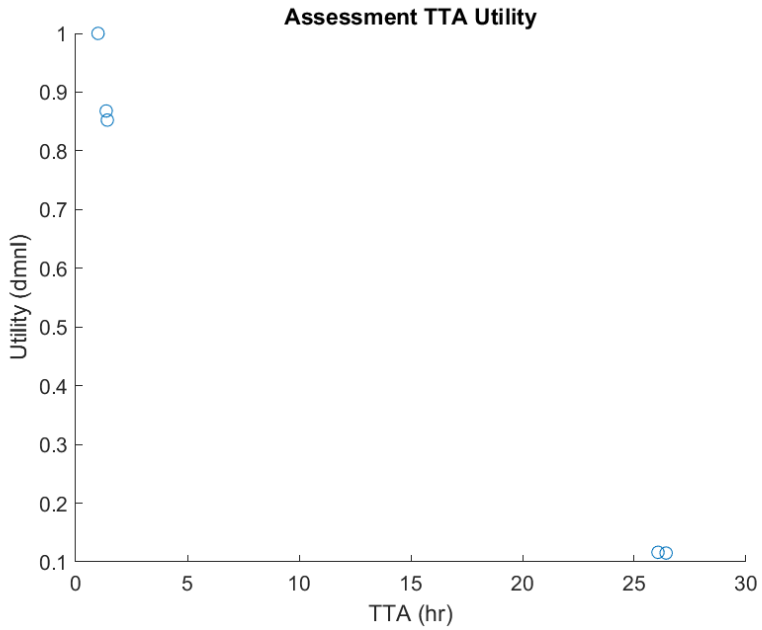

Figure A-19: Assessment TTA Utility

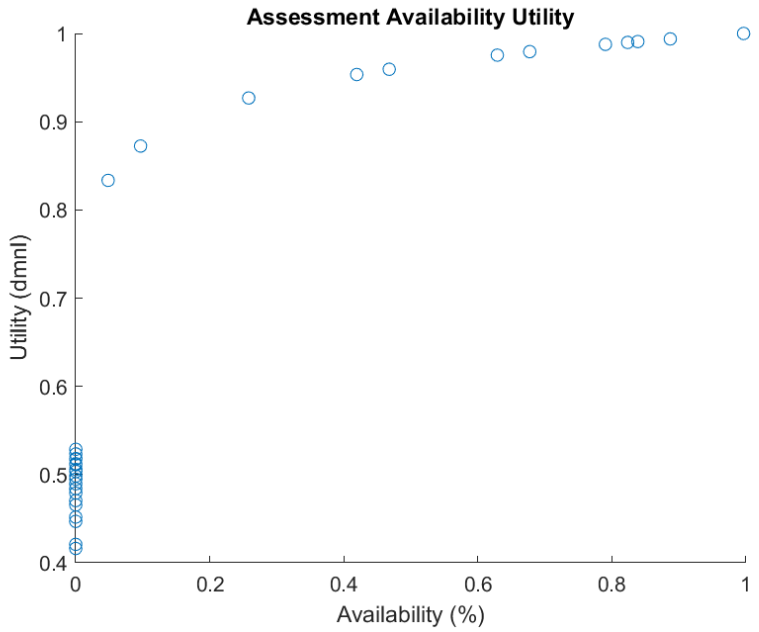

Figure A-20: Assessment Availability Utility

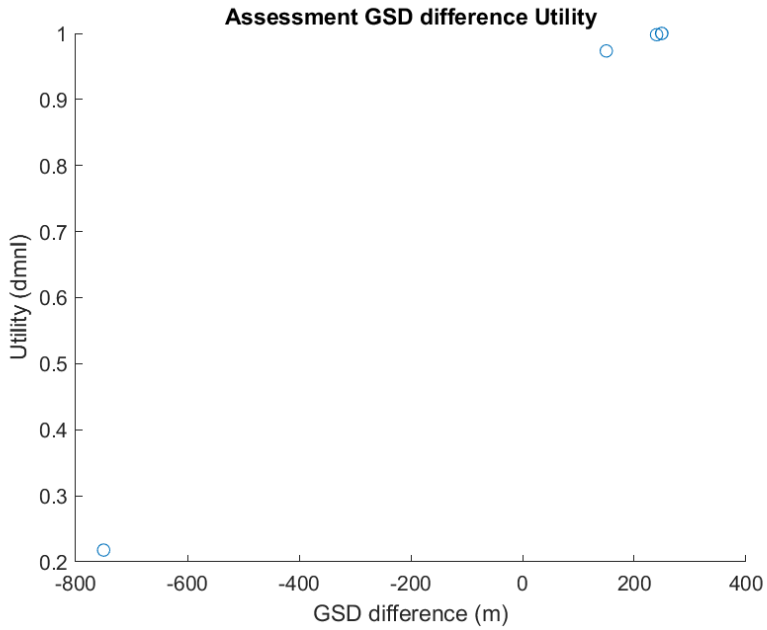

Figure A-21: Assessment GSD Utility

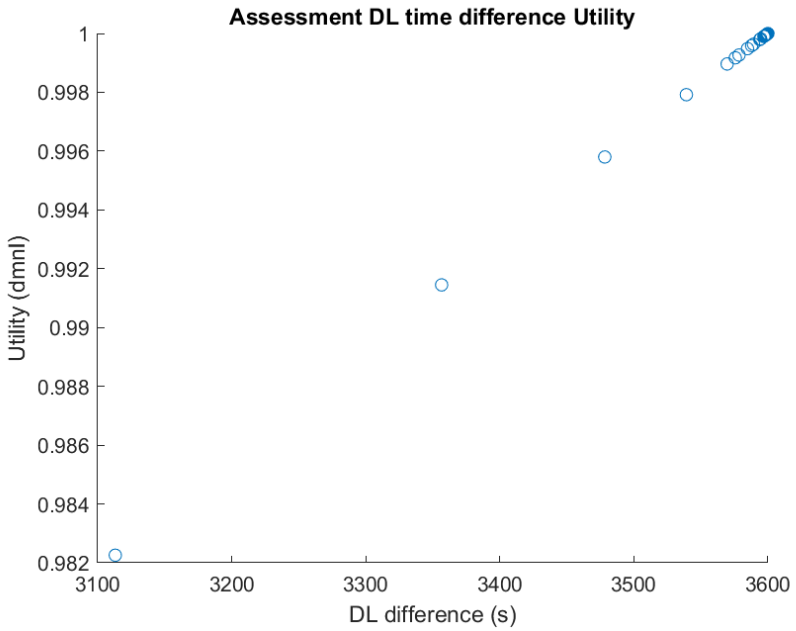

Figure A-22: Assessment DL Utility

Bibliography

[1] Air Force Drones Help California Firefighters Combat Wildfires. https://www.defense.gov/News/News-Stories/Article/Article/1348274/air-force-drones-help-california-firefighters-combat-wildfires/.

[2] Cooled versus uncooled cameras for long range surveillance. http://www.flirmedia.com/MMC/CVS/Tech_Notes/TN_0005_EN.pdf.

[3] DETECTORS ROICs and FPAs: Leading the Way in nBn and Digital Focal Plane Technology. https://www.lockheedmartin.com/content/dam/lockheed-martin/mfc/pc/focal-plane-arrays/mfc-sbf-detector-pc.pdf.

[4] FASMEE. https://www.fasmee.net/.

[5] Insitu Rapid Response Team Aids Wildfire Fighting Efforts. https://www.insitu.com/newsroom/story/insitus-rapid-response-team-aids-wildfire-fighting-efforts.

[6] Landsat 8 | U.S. Geological Survey. https://www.usgs.gov/landsat-missions/landsat-8.

[7] Landsat 8 Data Users Handbook | U.S. Geological Survey. https://www.usgs.gov/media/files/landsat-8-data-users-handbook.

[8] Mika Fire. https://www.mikafiresystem.com.

[9] Orbit - Sentinel 2 - Mission - Sentinel Online. https://dragon3.esa.int/web/sentinel/missions/sentinel-2/satellite-description/orbit.

[10] Remote Sensing Support for DOI Burn Area Emergency Response (BAER) Teams | Land Imaging Report Site. https://eros.usgs.gov/doi-remote-sensing-activities/2017/usgs/remote-sensing-support-doi-burn-area-emergency-response-baer-teams.

[11] Silicon Photodiodes Physics and Technology. https://www.univie.ac.at/photovoltaik/praktikum/ws2017/silicon_photodiodes.PDF.

[12] Suppression Costs | National Interagency Fire Center. https://www.nifc.gov/fire-information/statistics/suppression-costs.

[13] Systems of Systems (SoS) - SEBoK. https://www.sebokwiki.org/wiki/Systems_of_Systems_(SoS).

[14] USGS, EROS Offer Insights to National Fire Strategy Discussion | U.S. Geological Survey. https://www.usgs.gov/news/usgs-eros-offer-insights-national-fire-strategy-discussion.

[15] WO Staff Program - Burned Area Emergency Response BAER. https://www.fs.fed.us/naturalresources/watershed/burnedareas-wildland.shtml.

[16] Yarnell Hill Serious Accident Investigation Report | FRAMES. https://www.frames.gov/catalog/15735.

[17] Multi-Sensor Camera Systems for Long-Range Surveillance. https://www.infinitioptics.com/technology/multi-sensor, July 2016.

[18] Spreading like wildfire. *Nature Climate Change*, 7(11):755–755, November 2017.

[19] Teledyne Imaging Sensors H2RG™ Visible & Infrared Focal Plane Array. http://www.teledyne-si.com/products/Documents/H2RG%20Brochure%20-%20September%202017.pdf, September 2017.

[20] Work with the Difference Normalized Burn Index - Using Spectral Remote Sensing to Understand the Impacts of Fire on the Landscape. https://www.earthdatascience.org/courses/earth-analytics/multispectral-remote-sensing-modis/normalized-burn-index-dNBR/, March 2017.

[21] Camp Fire Rages in California. https://earthobservatory.nasa.gov/images/144225/camp-fire-rages-in-california, November 2018. Publisher: NASA Earth Observatory.

[22] Link Budget Calculations For A Satellite Link With An Electronically Steerable Antenna Terminal. https://www.kymetacorp.com/wp-content/uploads/2020/09/Link-Budget-Calculations-2.pdf, June 2019.

[23] NDVI FAQs: Top 23 Frequently Asked Questions About NDVI. https://eos.com/blog/ndvi-faq-all-you-need-to-know-about-ndvi/, August 2019.

[24] The Power of Real-Time Data for Firefighting. https://trajectorymagazine.com/the-power-of-real-time-data-for-firefighting/, June 2019.

[25] Fire Imaging Technologies for Wildland Fire Operations. https://www.nifc.gov/nicc/logistics/references/Fire%20Imaging%20Technologies%20Users%20Guide.pdf, February 2020.

[26] 2020 California wildfires. https://en.wikipedia.org/w/index.php?title=2020_California_wildfires&oldid=1025458072, May 2021. Page Version ID: 1025458072.

[27] List of large optical telescopes. https://en.wikipedia.org/w/index.php?title=List_of_large_optical_telescopes&oldid=1056176840, November 2021. Page Version ID: 1056176840.

[28] Osborne Fire Finder. https://en.wikipedia.org/w/index.php?title=Osborne_Fire_Finder&oldid=1033901342, July 2021. Page Version ID: 1033901342.

[29] Small telescope. https://en.wikipedia.org/w/index.php?title=Small_telescope&oldid=1034646852, July 2021. Page Version ID: 1034646852.

[30] Lukas Aichmayer, James Spelling, and Björn Laumert. Preliminary design and analysis of a novel solar receiver for a micro gas-turbine based solar dish system. *Solar Energy*, 114, April 2015.

[31] Robert S. Allison, Joshua M. Johnston, Gregory Craig, and Sion Jennings. Airborne Optical and Thermal Remote Sensing for Wildfire Detection and Monitoring. *Sensors*, 16(8):1310, August 2016. Number: 8 Publisher: Multidisciplinary Digital Publishing Institute.

[32] Panagiotis Barmpoutis, Periklis Papaioannou, Kosmas Dimitropoulos, and Nikos Grammalidis. A Review on Early Forest Fire Detection Systems Using Optical Remote Sensing. *Sensors*, 20(22):6442, January 2020. Number: 22 Publisher: Multidisciplinary Digital Publishing Institute.

[33] Timothy J. Brown, John D. Horel, Greg D. McCurdy, and Matthew G. Fearon. What is the Appropriate RAWS Network? page 103, August 2012.

[34] Charles S. Wasson. Trade Study Analysis of Alternatives. In *System Analysis, Design, and Development*, pages 672–690. John Wiley & Sons, Ltd, 2005. Section: 52 _eprint: https://onlinelibrary.wiley.com/doi/pdf/10.1002/0471728241.ch52.

[35] Chris at Infiniti Optics. Using Thermal Imaging To See Through Wildfire Smoke/Haze. https://www.youtube.com/watch?v=tTU3D81K5YM, September 2021.

[36] Edward Crawley. *System architecture : strategy and product development for complex systems*. Pearson Higher Education, Inc., Hoboken, NJ, 2016. Publication Title: System architecture : strategy and product development for complex systems.

[37] Swarvanu Dasgupta, John J Qu, and Xianjun Hao. Evaluating Remotely Sensed Live Fuel Moisture Estimations for Fire Behavior Predictions. page 10, 2005.

[38] Mark A. Finney. FARSITE: Fire Area Simulator-model development and evaluation. Technical Report RMRS-RP-4, U.S. Department of Agriculture, Forest Service, Rocky Mountain Research Station, Ft. Collins, CO, 1998.

[39] Rob Garner. Observatory - Optics. http://www.nasa.gov/content/goddard/hubble-space-telescope-optics-system, December 2017.

[40] Lee Ju Hyoung. Prediction of Large-Scale Wildfires With the Canopy Stress Index Derived from Soil Moisture Active Passive. *IEEE Journal of Selected Topics in Applied Earth Observations and Remote Sensing*, 14:2096–2102, 2021. Conference Name: IEEE Journal of Selected Topics in Applied Earth Observations and Remote Sensing.

[41] Kazuya Kaku. Satellite remote sensing for disaster management support: A holistic and staged approach based on case studies in Sentinel Asia. *International Journal of Disaster Risk Reduction*, 33:417–432, February 2019.

[42] D. E. Koelle. Specific transportation costs to GEO — past, present and future. *Acta Astronautica*, 53(4):797–803, August 2003.

[43] L3Harris Geospatial Solutions. Hot Mess: Remote Sensing Applications for Wildfires and Other Natural Disasters. https://www.youtube.com/watch?v=HCyaXcPKzEg, March 2021.

[44] James K. Lein. Environmental Sensing. In James K. Lein, editor, *Environmental Sensing: Analytical Techniques for Earth Observation*, pages 23–49. Springer, New York, NY, 2012.

[45] James K. Lein. Sensors and Systems. In *Environmental Sensing*, pages 51–81. Springer New York, New York, NY, 2012.

[46] Patrick Malone, Henry Apgar, Sherry Stukes, and Steve Sterk. Unmanned Aerial Vehicles unique cost estimating requirements. In *2013 IEEE Aerospace Conference*, pages 1–8, March 2013. ISSN: 1095-323X.

[47] Alexander Maranghides, Eric D. Link, Christopher U. Brown, William Mell, Steven Hawks, Mike Wilson, Will Brewer, Robert Vihnanek, and William D. Walton. A Case Study of the Camp Fire - Fire Progression Timeline. February 2021. Last Modified: 2021-03-01T01:03-05:00.

[48] Robert Margetta. NASA Awards Launch Services Contract for GOES-U Mission. http://www.nasa.gov/press-release/nasa-awards-launch-services-contract-for-goes-u-mission, September 2021.

[49] Aden B. Meinel. Cost Scaling Laws Applicable To Very Large Optical Telescopes. In David L. Crawford, editor, *Instrumentation in Astronomy III*, volume 0172, pages 2 – 7. SPIE, 1979. Backup Publisher: International Society for Optics and Photonics.

[50] Tom Mellin. National Infrared Operations Update. https://appliedsciences.nasa.gov/sites/default/files/2019-09/1_3_Mellin_NIROPS_4_TFRSAC_Spring19.pdf.

[51] Ontario Forest Fires. #DYK there are 3 types of wildland fires? Ground fires burn just below the surface. Surface fires burn in the vegetation layer that litters the forest floor. Crown fires burn in the tree tops. For general information about #wildlandfires, visit http://ontario.ca/forestfire. https://t.co/GlQ07JLB37. `https://twitter.com/onforestfires/status/1102634466831409153`, March 2019.

[52] Sung Wook Paek, Sangtae Kim, and Olivier de Weck. Optimization of Reconfigurable Satellite Constellations Using Simulated Annealing and Genetic Algorithm. *Sensors (Basel, Switzerland)*, 19(4):765, February 2019.

[53] Carlton Pennypacker, Marek Jakubowski, Maggi Kelly, Michael Lampton, Christopher Schmidt, Scott Stephens, and Robert Tripp. FUEGO — Fire Urgency Estimator in Geosynchronous Orbit — A Proposed Early-Warning Fire Detection System. *Remote Sensing*, 5(10):5173–5192, October 2013.

[54] Sjoukje Y. Philip, Sarah F. Kew, Geert Jan van Oldenborgh, Faron S. Anslow, Sonia I. Seneviratne, Robert Vautard, Dim Coumou, Kristie L. Ebi, Julie Arrighi, Roop Singh, Maarten van Aalst, Carolina Pereira Marghidan, Michael Wehner, Wenchang Yang, Sihan Li, Dominik L. Schumacher, Mathias Hauser, Rémy Bonnet, Linh N. Luu, Flavio Lehner, Nathan Gillett, Jordis Tradowsky, Gabriel A. Vecchi, Chris Rodell, Roland B. Stull, Rosie Howard, and Friederike E. L. Otto. Rapid attribution analysis of the extraordinary heatwave on the Pacific Coast of the US and Canada June 2021. preprint, Earth system change: climate scenarios, November 2021.

[55] Francisco Castro Rego, Penelope Morgan, Paulo Fernandes, and Chad Hoffman. *Fire Science: From Chemistry to Landscape Management*. Springer Textbooks in Earth Sciences, Geography and Environment. Springer International Publishing, Cham, 2021.

[56] Robert A. Schowengerdt. CHAPTER 1 - The Nature of Remote Sensing. In Robert A. Schowengerdt, editor, *Remote Sensing (Third Edition)*, pages 1–X. Academic Press, Burlington, January 2007.

[57] H. Philip Stahl. Survey of cost models for space telescopes. *Optical Engineering*, 49(5):053005–053005, 2010. Place: BELLINGHAM Publisher: SPIE-SOC PHOTO-OPTICAL INSTRUMENTATION ENGINEERS.

[58] Emanuel Arnal Storey, Krista R. Lee West, and Douglas A. Stow. Utility and optimization of LANDSAT-derived burned area maps for southern California. *International Journal of Remote Sensing*, 42(2):486–505, January 2021. Publisher: Taylor & Francis.

[59] Ricardo Valerdi. Cost Metrics for Unmanned Aerial Vehicles. In *Infotech@Aerospace*, Infotech@Aerospace Conferences. American Institute of Aeronautics and Astronautics, September 2005.

[60] C. Vázquez Garcìa, I. Pérez Garcilópez, P. Contreras Lallana, B. Vinouze, and B. Fracasso. Liquid crystal optical switches. In Baojun Li and Soo Jin Chua, editors, *Optical Switches*, Woodhead Publishing Series in Electronic and Optical Materials, pages 206–240. Woodhead Publishing, January 2010.

[61] James Richard Wertz, David F Everett, and Jefferey John Puschell. *Space mission engineering : the new SMAD*. Space technology library ; v. 28. Microcosm Press, Hawthorne, Calif, 2011. Publication Title: Space mission engineering : the new SMAD.

[62] Edgar Zapata. The State of Play US Space Systems Competitiveness: Prices, Productivity, and Other Measures of Launchers & Spacecraft. October 2017. Number: KSC-E-DAA-TN48988.